Iranian Journal of Science and Technology, Transactions of Civil Engineering
https://doi.org/10.1007/s40996-026-02178-0

RESEARCH PAPER

Durability of self-compacting concrete with micro-Silica and metakaolin Under freeze–Thaw cycles in sulfate and chloride environments

Yaghoub Mohammadi[1] · Arian DarvishaliNezhad[1] · Husain Khalaf Jarallah[2]

Received: 18 August 2025 / Accepted: 16 May 2026

Abstract
This study examines the durability of self-compacting concrete (SCC) in sulfate and chloride environments subjected to freeze–thaw cycles by incorporating micro-silica and metakaolin. While prior research has explored the individual effects of micro-silica or metakaolin on concrete durability, the combined influence of these supplementary cementitious materials under simultaneous freeze–thaw, sulfate, and chloride exposure remains underexplored, representing a critical gap that this study addresses as its primary innovation. The research identifies an effective mix proportion (3% micro-silica and 7.5% metakaolin, Mi3Mt7.5), which improves compressive strength, stiffness, and resistance to weight loss compared to additive-free mixes or those with higher additive dosages. These enhancements result from reduced porosity and a denser cement matrix, as confirmed by scanning electron microscopy (SEM) analysis, which showed reduced deterioration in sulfate environments. The Mi3Mt7.5 mix outperformed other compositions, particularly in chloride environments, making it suitable for structures in cold and corrosive settings, such as marine constructions and pavements exposed to de-icing salts. Furthermore, the incorporation of these supplementary cementitious materials promotes sustainability by reducing cement consumption and associated CO_2 emissions, contributing to environmentally friendly concrete production. However, the study did not include chloride diffusion or sulfate expansion tests, which could further clarify the long-term performance of these mixes. This research provides practical insights for designing durable concrete and contributes to engineering standards for challenging environments, serving as a reference for improving the longevity and sustainability of concrete structures.

Keywords Self-compacting concrete (SCC) · Micro-silica · Supplementary cementitious materials · Sulfate environment · Chloride environment · Durability index

1 Introduction

Self-compacting concrete (SCC) is an advanced concrete technology that flows and consolidates under its own weight without requiring mechanical vibration. However, SCC faces challenges in harsh environments, including deterioration from freeze–thaw cycles, penetration of chloride and sulfate ions, and reduced durability due to relatively high porosity, which can lead to cracking, loss of compressive strength, and degradation of the cement matrix (Bhavani and Saravanan 2023). The incorporation of pozzolanic additives such as micro-silica (silica fume) and metakaolin into SCC formulations significantly enhances the material's durability properties (Mousavi et al. 2021). These pozzolanic additives react with calcium hydroxide produced during cement

✉ Yaghoub Mohammadi
yaghoubm@uma.ac.ir

Arian DarvishaliNezhad
arian.darvishalinezhad@uma.ac.ir

Husain Khalaf Jarallah
khalfdce@uomustansiriyah.edu.iq

[1] Department of Civil Engineering, Faculty of Engineering, University of Mohaghegh Ardabili, Ardabil, Iran

[2] Department of Civil Engineering, College of Engineering, Mustansiriyah University, Baghdad, Iraq

Published online: 09 June 2026

hydration to form additional calcium silicate hydrate (C-S-H) gel, which densifies the concrete matrix and reduces permeability (Luan et al. 2023). These pozzolanic reactions, by reducing capillary porosity and improving paste-aggregate bonding, enhance SCC's resistance to physical deterioration from freeze–thaw cycles and chemical attack from sulfate and chloride ion penetration (Abbas and Muntean 2025). Furthermore, these materials contribute to sustainability by partially replacing Portland cement, thereby lowering the carbon footprint associated with cement production, which accounts for approximately 8% of global CO_2 emissions (He et al. 2024).

In harsh environmental conditions, such as marine structures and pavements exposed to de-icing salts, where concrete is subjected to combined freeze–thaw cycles and aggressive chemical environments containing sulfates and chlorides, the enhanced microstructure provided by these mineral admixtures is critical for long-term performance (Wang et al. 2025). Although prior studies have investigated the individual effects of micro-silica or metakaolin on SCC durability under specific conditions, such as freeze–thaw cycles or chemical attacks, the synergistic effects of their combined use under simultaneous exposure to freeze–thaw, sulfate, and chloride environments remain largely underexplored (Penna et al. 2022). This research gap, critical for real-world applications like marine constructions and pavements, forms the core innovation of this study, which focuses on the performance of the ternary system (micro-silica, metakaolin, and SCC). The durability of SCC systems with micro-silica and metakaolin under such combined exposure conditions involves complex interactions between physical deterioration mechanisms from freeze–thaw cycles and chemical deterioration from ion penetration and subsequent reactions within the concrete matrix (Khosravi et al. 2025).

Metakaolin, a highly effective pozzolanic admixture, fundamentally improves the durability characteristics of self-compacting concrete through microstructural enhancement. Incorporating metakaolin significantly reduces concrete porosity and refines the pore structure, directly translating to improved resistance against multiple deterioration mechanisms (Malaiškienė and Jakubovskis 2025). This densification effect occurs through the pozzolanic reaction between metakaolin and calcium hydroxide, forming additional calcium silicate hydrate gel that fills voids and creates a more impermeable matrix (Zhao et al. 2024). Derived from calcined kaolin clay, metakaolin also offers environmental benefits by reducing reliance on clinker-based cement and minimizing CO_2 emissions during production (Xiong et al. 2023). The enhanced pore structure provided by metakaolin delivers substantial improvements in freeze–thaw resistance. Research demonstrates that metakaolin-containing SCC can achieve high freeze–thaw resistance grades, with some formulations reaching F600 performance through the synergistic action of metakaolin with other concrete components (Yan 2024). This improvement results from reduced mean pore size, which prevents the absorption of liquid water and blocks subsequent freezing and expansion damage (Li et al. 2022). Studies confirm that metakaolin incorporation leads to excellent freeze–thaw resistance with less than 5% mass loss even after extensive cycles (Chen et al. 2024). In chemical attack environments, metakaolin exhibits exceptional performance against both chloride and sulfate exposure. Replacing cement with metakaolin significantly reduces chloride penetrability and substantially improves concrete durability in sulfate-chloride environments (Tuncer et al. 2025). This improved resistance is inversely correlated with the replacement level, meaning higher metakaolin contents generally provide better protection (Chithra 2022). The selection of a 7.5% metakaolin dosage in this study is based on prior literature, which indicates that dosages between 5% and 10% achieve an optimal balance between pozzolanic reactivity, pore refinement, and workability retention, avoiding adverse effects of higher dosages such as increased viscosity and reduced compaction (Moceikis et al. 2020). At 7.5%, metakaolin maximizes the formation of stable C-A-H phases that suppress deleterious expansions in sulfate environments while maintaining fresh-state flowability essential for SCC, as evidenced by rheological tests in this study (Chithra 2022). Additionally, metakaolin-enhanced SCC exhibits lower gas permeability compared to reference concrete mixtures, further reducing ingress pathways for aggressive ions (Li et al. 2020). The durability benefits of metakaolin extend to various curing conditions, with research showing that SCC containing metakaolin maintains superior freeze–thaw durability and chloride penetration resistance even when cured at low temperatures (Zhagifarov et al. 2024).

Micro-silica, also known as silica fume, exhibits complex and dosage-dependent effects on the durability of self-compacting concrete, particularly under freeze–thaw conditions. Research indicates that at lower dosages (2.5–5%), micro-silica can negatively affect freeze–thaw durability, with some studies reporting severe deterioration after just two freeze–thaw cycles and increased surface mass loss up to 67 g/m² (González-Sánchez et al. 2020). However, higher dosages (7.5%) demonstrate improved performance, showing no visible surface flaws and enhanced resistance against freeze–thaw cycles, attributed to an air-entraining effect (Moceikis et al. 2020). The beneficial effects of micro-silica at appropriate dosages stem from its pozzolanic reaction with calcium hydroxide, producing additional C-S-H phases that strengthen the fiber-matrix bond and improve overall durability (Moceikis et al. 2020). As a by-product of silicon production, micro-silica also advances sustainability by diverting industrial waste from landfills and reducing CO_2 emissions through cement replacement (Abbas and Muntean 2025). When properly incorporated, micro-silica significantly reduces concrete porosity and improves resistance to both chloride ion penetration and freeze–thaw cycles, similar to metakaolin's effects (Abbas and Muntean 2025). This durability enhancement occurs through porosity reduction and pore structure refinement, minimizing water ingress and subsequent freeze–thaw damage (Abbas and Muntean 2025). Studies show that high-performance concrete compositions containing micro-silica achieve high freeze–thaw resistance prediction coefficients, indicating superior long-term performance (Malaiškienė and Jakubovskis 2025). The key to successful micro-silica application lies in optimizing the dosage to achieve beneficial pozzolanic effects while avoiding adverse impacts observed at suboptimal concentrations (Moceikis et al. 2020).

The freeze–thaw performance of self-compacting concrete with mineral admixtures exhibits distinct patterns depending on the type and dosage of supplementary cementitious materials. Metakaolin consistently demonstrates superior freeze–thaw resistance across various applications, even when cured at low temperatures (Bumanis and Bajare 2017). This improvement occurs through reduced mean pore size, which prevents liquid water absorption and blocks subsequent freezing and expansion damage (González-Sánchez et al. 2020). Optimal metakaolin dosages for freeze–thaw resistance fall within the 2.5–5% replacement range, where maximum surface mass loss remains below 50 g/m² even after 112 freeze–thaw cycles with de-icing salt (Moceikis et al. 2020). However, excessive metakaolin content (7.5%) can lead to significant surface deterioration with mass loss reaching 465 g/m², highlighting the importance of dosage control (Moceikis et al. 2020). High-performance compositions can achieve exceptional freeze–thaw resistance grades, such as F600, through the synergistic action of metakaolin with plasticizers and water-repelling agents (Bogdanov and Mavlyuberdinov 2020). This enhanced performance results from increased concrete density, reduced water-cement ratios, and the formation of low-base calcium hydro silicates that remain stable under cyclic freeze–thaw effects (Bogdanov and Mavlyuberdinov 2020). Advanced concrete formulations with properly proportioned mineral admixtures demonstrate remarkable durability, maintaining less than 5% mass loss even after extensive freeze–thaw cycles (Abbas and Muntean 2025). The combination of reduced porosity and refined pore structure in ternary mixtures creates more compact concrete that is less susceptible to freeze–thaw damage, thereby increasing service life under adverse environmental conditions (Dhabhai and Shekhawat 2020). These admixtures not only enhance performance but also support sustainable construction practices by reducing cement usage and CO_2 emissions (Balamuralikrishnan and Saravanan 2021).

The chemical resistance of self-compacting concrete containing metakaolin and micro-silica under sulfate and chloride exposure demonstrates significant protective benefits of these mineral admixtures. Replacing cement with metakaolin effectively enhances concrete resistance to chloride attack and substantially improves durability in combined sulfate-chloride environments compared to conventional concrete (Abbas et al. 2010). This enhanced performance stems from the pozzolanic reaction that creates additional binding phases and reduces permeability pathways for aggressive ion penetration (Chithra 2022). Long-term exposure studies confirm the effectiveness of these mineral admixtures against chemical attacks, with high-performance concrete formulations containing metakaolin showing better resistance to chloride and sulfate attacks over exposure periods of up to 180 days (Patel and Shah 2013). The replacement of cement with metakaolin significantly reduces chloride penetrability, with higher replacement levels generally providing enhanced protection (Chithra 2022). These durability improvements correlate directly with microstructural changes in the concrete matrix, with lower porosities measured at various metakaolin replacement levels and sorptivity showing an inverse correlation with the replacement level (Chithra 2022). Metakaolin-enhanced SCC generally exhibits lower gas permeability compared to reference concrete mixtures, reducing ingress pathways for sulfate and chloride ions (Li et al. 2020). These protective effects extend to various exposure scenarios and curing conditions, with SCC containing metakaolin-containing waste demonstrating excellent resistance to chloride penetration even when cured at low temperatures (Bumanis and Bajare 2017). Advanced concrete formulations incorporating both metakaolin and micro-silica work synergistically to reduce porosity and refine pore structure, creating multiple barriers against chemical ingress (Abbas and Muntean 2025). Research on sulfate resistance specifically shows that optimal mineral admixture combinations can reduce magnesium sulfate attack by one-third compared to control mixtures (Khosravi et al. 2025).

This study examines the durability of self-compacting concrete (SCC) in sulfate and chloride environments subjected to freeze–thaw cycles by incorporating micro-silica and metakaolin. While prior research has explored the individual effects of micro-silica or metakaolin on concrete durability, the combined influence of these supplementary cementitious materials (SCMs) under simultaneous freeze–thaw, sulfate, and chloride exposure remains underexplored, representing a critical gap that this study addresses (Penna et al. 2022; Khosravi et al. 2025; Malaiškienė and Jakubovskis

2025; Zhao et al. 2024; Xiong et al. 2023; Yan 2024; Li et al. 2022; Chen et al. 2024; Tuncer et al. 2025; Chithra 2022; Moceikis et al. 2020; Li et al. 2020; Zhagifarov et al. 2024; González-Sánchez et al. 2020; Bumanis and Bajare 2017; Bogdanov and Mavlyuberdinov 2020; Dhabhai and Shekhawat 2020; Balamuralikrishnan and Saravanan 2021; Abbas et al. 2010; Patel and Shah 2013; Ezhilarasi 2020; Liu et al. 2021). The research identifies an effective mix proportion (3% micro-silica and 7.5% metakaolin, Mi3Mt7.5), which improves compressive strength, stiffness, and resistance to weight loss compared to additive-free mixes or those with higher additive dosages. These enhancements result from reduced porosity and a denser cement matrix, as confirmed by scanning electron microscopy (SEM) analysis, which showed reduced deterioration in sulfate environments. The Mi3Mt7.5 mix outperformed other compositions, particularly in chloride environments, with a compressive strength of 62.29 MPa, a dynamic modulus of elasticity of 45.62 GPa after 150 freeze–thaw cycles, and a weight loss of only 0.13% in a chloride environment, making it suitable for structures in cold and corrosive settings, such as marine constructions and pavements exposed to de-icing salts. SEM analysis further confirmed reduced ettringite crystal formation and a denser microstructure. Furthermore, the incorporation of these SCMs promotes sustainability by reducing cement consumption and associated CO_2 emissions, contributing to environmentally friendly concrete production (He et al. 2024; Wang et al. 2025; Penna et al. 2022; Khosravi et al. 2025; Malaiškienė and Jakubovskis 2025; Zhao et al. 2024; Xiong et al. 2023; Yan 2024; Li et al. 2022; Chen et al. 2024; Tuncer et al. 2025; Chithra 2022; Moceikis et al. 2020; Li et al. 2020; Zhagifarov et al. 2024; González-Sánchez et al. 2020; Bumanis and Bajare 2017; Bogdanov and Mavlyuberdinov 2020; Dhabhai and Shekhawat 2020; Balamuralikrishnan and Saravanan 2021; Abbas et al. 2010; Patel and Shah 2013; Ezhilarasi 2020; Liu et al. 2021; Müller et al. 2021). However, the study did not include chloride diffusion or sulfate expansion tests, which could further clarify the long-term performance of these mixes.

Recent research has highlighted the potential of alternative supplementary cementitious materials, such as fly ash, ground granulated blast furnace slag (GGBFS), and rice husk ash, in geopolymer-based self-compacting concrete, achieving sustainability benefits through enhanced microstructural properties and reduced environmental impact (Thatikonda et al. 2024; Naresh et al. 2025). Advanced statistical optimization and performance evaluation of self-compacting geopolymer concrete utilizing industrial by-products have enabled the achievement of superior mechanical and durability properties (Naresh et al. 2025). Micro-silica, as a partial replacement for fly ash and GGBFS in geopolymer-based SCC, has demonstrated improved compressive strength and durability (Thatikonda et al. 2024). Additionally, hybrid machine learning models enhanced with Gaussian noise augmentation have been developed to predict the strength of metakaolin-based geopolymer concrete, demonstrating the potential to improve sustainable mix designs through predictive analytics (Abdellatief et al. 2025). Recent reviews of geopolymer foam concrete have emphasized the role of pore characteristics and compressive strength in durability, alongside the application of artificial intelligence for simulating geopolymer foam concrete strength to support sustainable mix designs (Abdellatief et al. 2025). Deep learning models have also been developed to predict surface chloride concentration in marine tidal zones, further enhancing durability assessments in chloride environments (Abdellatief et al. 2025). These advancements underscore the potential of combining advanced materials and computational technologies to optimize concrete design. This study provides practical insights for designing durable concrete through comprehensive experimental data and rigorous analyses, contributing to the development of engineering standards for challenging environments and serving as a reference for improving the longevity and sustainability of concrete structures.

The experimental program was designed to evaluate the durability of self-compacting concrete (SCC) incorporating micro-silica and metakaolin under combined freeze–thaw, sulfate, and chloride exposure. The methodology encompassed mix design, specimen preparation, curing, and testing under controlled environmental conditions. To provide a clear overview of the experimental procedure, a flowchart is presented in Fig. 1, summarizing the key steps from material selection to data analysis. The flowchart in Fig. 1 illustrates the sequence of these steps, including material preparation, specimen casting, curing, exposure conditions, testing protocols, and data analysis, ensuring clarity for readers in understanding the experimental workflow.

2 Materials

2.1 Aggregates

Natural aggregates with normal weight were sourced from the Ghizildash mine in Namin (Kulan Darreh village). The aggregates, of siliceous composition, comprised crushed gravel (maximum size 12.5 mm) and natural sand (maximum size 4.75 mm, fineness modulus 2.9). Aggregate gradation was conducted per ASTM C136 (2020) and compared with ASTM C33 (2023), confirming compliance with standard limits (Figs. 2 and 3).

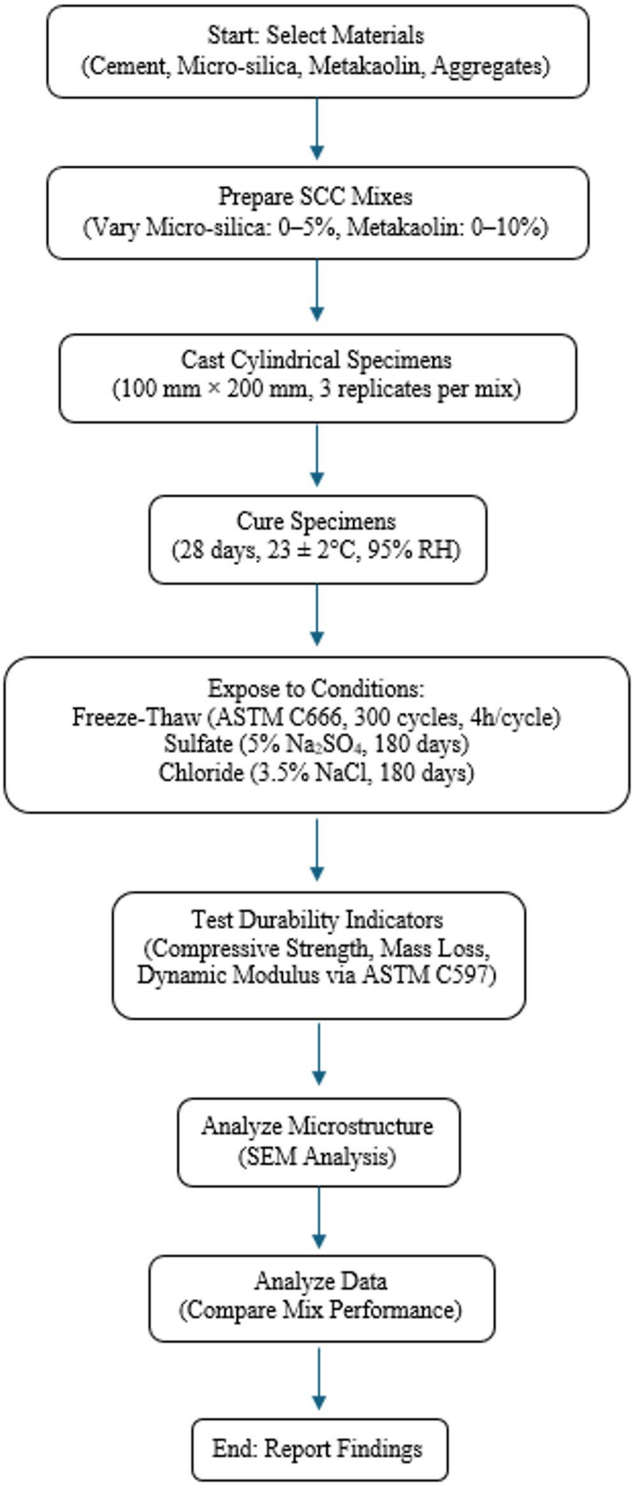

Fig. 1 Flowchart of the experimental program for evaluating SCC durability

2.2 Superplasticizer

To enhance workability and reduce the water-to-cement ratio, a naphthalene sulfonate-based superplasticizer (Fabcrete-100) from Fiber Company, compliant with ASTM C494 (2024), was used. This admixture increases early and ultimate concrete strength and is suitable for self-consolidating concrete. Additionally, to create a sulfate environment, powdered magnesium sulfate from Tehran Acid Company was employed. The technical specifications of these chemical admixtures are presented in Table 1.

2.3 Air-Entraining Admixture

Sure Air 800, an air-entraining admixture from Shurair Company, compliant with ASTM C260 (2025), was incorporated to generate microscopic air bubbles, enhancing concrete durability against freeze–thaw cycles. This admixture mitigates pressures from water freezing, significantly improving concrete stability (Table 2).

2.4 Water

The mixing water used for preparing and curing self-compacting concrete (SCC) was potable water from Ardabil, compliant with ASTM D1129 standards (ASTM D1129-13 2024). Free of undesirable taste or odor, this water was suitable for SCC production.

2.5 Cement

Portland pozzolanic cement from the Ardabil Cement Factory, with a density of 3130 kg/m³ (corresponding to a specific gravity of 3.13), was used. The chemical composition of this cement is presented in Table 3.

2.6 Metakaolin

The metakaolin used in this study, sourced from the Delijan factory, is a nearly white powder with a density of 2600 kg/m³ (corresponding to a specific gravity of 2.6). Its chemical composition is provided in Table 3.

2.7 Micro-Silica Gel

This study utilized micro-silica gel as an additive in self-compacting concrete (SCC). This material enhances compressive, tensile, and flexural strengths, reduces plastic shrinkage cracks, and improves durability against permeability and cyclic dynamic loads. The physical properties of the micro-silica gel are presented in Table 4, and its chemical composition is detailed in Table 3.

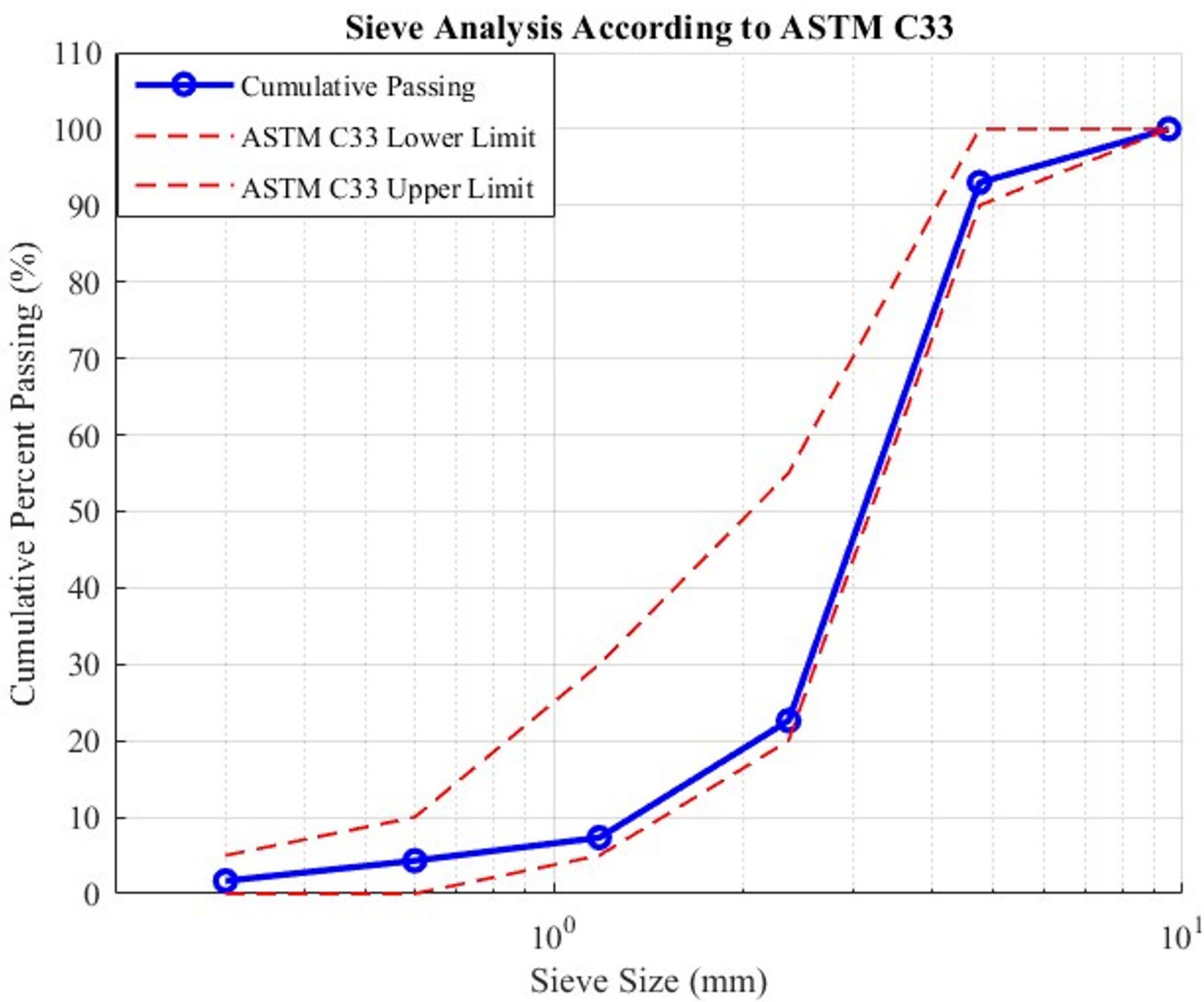

Fig. 2 Gradation curve of coarse aggregates compared to ASTM C33 (2023)

2.8 Los Angeles Abrasion Test

The Los Angeles abrasion test was conducted to assess the abrasion resistance of coarse aggregates smaller than 37.5 mm. Aggregates and steel balls were placed in a rotating steel drum, where abrasion occurred due to impact and movement during rotation. According to ASTM C131-89 (2020) and ASTM C535 (2024), Method C was selected based on aggregate gradation (Table 5) and the number and weight of steel balls were determined from Table 6. After 500 rotations, the material was sieved through a No. 12 sieve and the abrasion percentage was calculated using the following equation:

$$\text{Abrasion Percentage} = \left(\frac{\text{Weight of material passing No. 12 sieve}}{\text{Total weight of material}}\right) \times 100 \qquad (1)$$

The test yielded an abrasion percentage of 19.68%. This value is well within the acceptable range for high-quality aggregates used in durable concrete, as ASTM C33 (2023) recommends a maximum abrasion loss of 50% for coarse aggregates in structural concrete, with values below 30% typically indicating superior resistance to mechanical degradation. The obtained 19.68% abrasion loss reflects the robust nature of the siliceous aggregates sourced from the Ghizildash mine, suggesting excellent resistance to wear and fragmentation under cyclic loading or freeze–thaw conditions. This low abrasion loss contributes to the durability of SCC, particularly in harsh environments like pavements exposed to de-icing salts or marine structures, by minimizing aggregate breakdown and maintaining matrix integrity, as supported by prior studies showing that aggregates with abrasion losses below 20% enhance long-term concrete

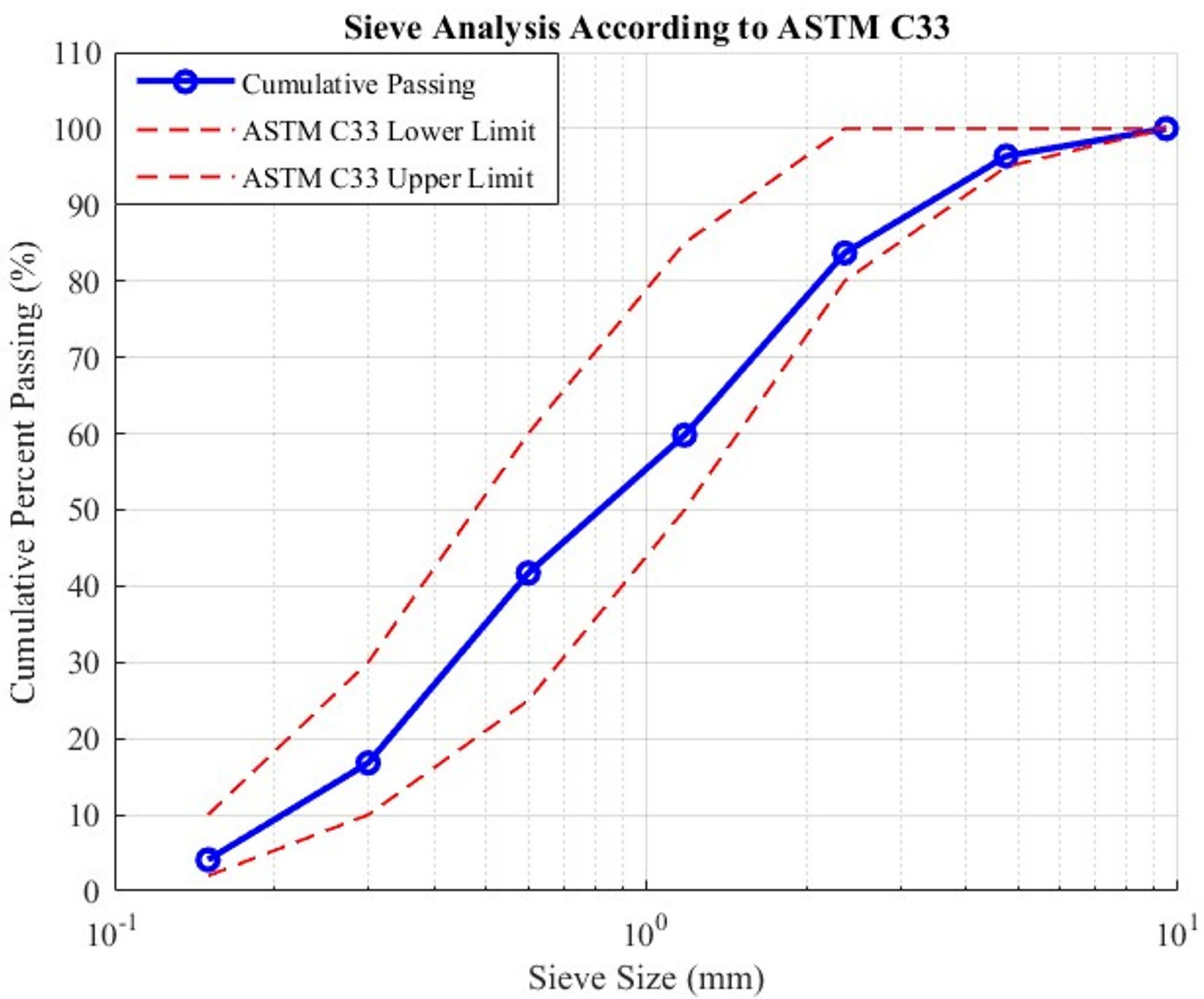

Fig. 3 Gradation curve of fine aggregates compared to ASTM C33 (2023)

Table 1 Technical specifications of chemical admixtures

Material	Appearance	Color	Density	pH	Chloride Content	Flammability	Freezing Point (°C)	Solubility (g/L)	Iron Content (%)	Decomposition Temperature (°C)
Fabcrete-100 Superplasticizer	Semi-Viscous Liquid	Dark Brown	1.112 kg/L	7.1	None	None	0	–	–	–
Magnesium Sulfate	Crystalline	White	2.45 g/cm³	7	0.002%	–	–	36	0.001%	1124

Table 2 Technical specifications of sure air 800 air-entraining admixture

Property	Specific gravity (g/cm³)	pH	Color	Fluoride content	Flammability	Freezing point (°C)
Value	1.04 g/cm³	10–11	Amber	None-Fluoride	Non-Flammable	−1 °C

Table 3 Chemical composition of cementitious materials

Material	SiO_2 (%)	Al_2O_3 (%)	Fe_2O_3 (%)	CaO (%)	MgO (%)	Na_2O (%)	K_2O (%)	P_2O_5 (%)	SO_3 (%)	Cl (%)	C (%)	SiC (%)	H_2O (%)	TiO_2 (%)
Portland Pozzolanic Cement	26.85	6.5	3.20	56.50	> 5	0.44	1.10	–	> 1	< 5	–	–	–	–
Micro-silica	96.4	1.32	0.87	0.49	0.97	0.31	1.01	0.16	0.10	0.04	0.3	0.5	0.08	–
Metakaolin	80.76	15.69	0.04	1.46	0.05	0.01	0.04	0.10	0.12	–	–	–	–	0.38

performance (Malaiškienė and Jakubovskis 2025; Balamuralikrishnan and Saravanan 2021).

2.9 Water Absorption Test

The water absorption test for coarse and fine aggregates was conducted per ASTM C127 (2025) and ASTM C128 standards (2025). Samples of 1000 g of sand and gravel were submerged in water for 24 h. After removal, the surface moisture was dried using warm air, and their weights were recorded as 1056 g for sand and 1017 g for gravel. The total moisture content (P) and water absorption (E) were calculated using Eqs. (2) and (3), respectively:

$$P = \frac{(B - C)}{(C - A)} \times 100 \tag{2}$$

$$P = \frac{(D - C)}{(C - A)} \times 100 \tag{3}$$

where P is the total moisture content (%), E is the water absorption (%), B is the weight of the container and wet sample, C is the weight of the container and dry sample, D is the weight of the container and saturated surface-dry sample and A is the weight of the container. The results indicated a total moisture content of 0.4% and water absorption of 1.6% for gravel and 2.95% and 3.05% for sand, respectively.

2.10 Mix Design

The selection of materials and mix proportions is critical for achieving self-compacting concrete (SCC) with optimal properties, as these directly influence cost and performance. In this study, the absolute volume method was employed for mix design. The fine-to-coarse aggregate ratio was set at 60:40, and superplasticizer use was minimized for cost efficiency. The superplasticizer dosage was fixed at 9 g/m³ across all mix designs to maintain consistency in comparing the effects of micro-silica and metakaolin on fresh and hardened concrete properties, as varying superplasticizer content could confound the pozzolanic contributions of these additives. Similarly, the air-entraining admixture (Fabair-200) was fixed at 0.9 g/m³ across all mixes to ensure consistent air content (approximately 4–6% as per ASTM C231 (2026), which is critical for freeze–thaw resistance by providing controlled air voids to accommodate hydraulic pressure from ice expansion (Tuncer et al. 2025; Patel and Shah 2013). This dosage was selected based on preliminary tests and EFNARC guidelines (EN 2009), ensuring adequate air entrainment without compromising workability or strength, particularly in pozzolan-rich mixes where high metakaolin levels (e.g., 15%) increase viscosity and could reduce air

Table 4 Physical Properties of Micro-silica Gel

Color	Physical state	Chloride content	Nitrate	Freezing point	Flash point	Density (kg/m³)
Gray	Gel-like at rest, liquid upon agitation	Free of chloride or below standard limits	None	0 °C	None	1350

Table 5 Los Angeles test methods based on gradation

Passing (mm)	Retained (mm)	Sample Weight (g) - Methods			
		A	B	C	D
37.5	25	1250 ± 25			
25	19	1250 ± 25			
19	12.5	1250 ± 25	2500 ± 25		
12.5	9.5	1250 ± 25	2500 ± 10		
9.5	6.3			2500 ± 10	
6.3	4.75			2500 ± 10	
4.75 (No.4)	2.36 (No.8)				5000 ± 10

Table 6 Number and weight of steel balls

Test method	Number of balls	Total weight of balls (g)
A	12	5000 ± 25
B	11	4585 ± 25
C	8	3330 ± 25
D	6	2500 ± 25

void stability (Chithra 2022; Ashteyat et al. 2024). The fixed air-entraining dosage minimizes variability in air content, allowing the study to isolate the effects of micro-silica and metakaolin on durability, though potential interactions with pozzolans, such as reduced air void formation in high-viscosity mixes like Mi3Mt15, are discussed in Sect. 4.6. The optimal mix was selected based on workability and fresh concrete properties. Following Okamura and Ouchi's method (Okamura and Ouchi 2003), water-to-powder ratios and mix components were determined. Various water-to-cement ratios were evaluated across four mix designs. The highest 7-day compressive strength was achieved at a 40% water-to-cement ratio; however, due to unsatisfactory self-compacting properties, the 45% ratio was selected as the optimal mix. The mix proportions, compliant with ACI 211 − 89 (1977), are presented in Table 7.

In Table 7, Mi denotes micro-silica and Mt denotes metakaolin. The subscript numbers indicate the percentage of these materials relative to cement. The selection of 7.5% metakaolin as the primary dosage in the optimized mix (Mi3Mt7.5) was informed by dosage-dependent effects reported in the literature, where this level provides an effective balance between pozzolanic reactivity—enhancing C-S-H and C-A-H formation—and rheological performance, avoiding the adverse viscosity increases observed at 15% that compromise self-compaction and introduce microstructural voids (Chithra 2022; Ashteyat et al. 2024; Kabay and Tufekci 2016). This choice was validated through preliminary trials, confirming improved compressive strength and reduced porosity without segregation risks, though the fixed superplasticizer dosage constrained optimal flow in high-metakaolin mixes, as discussed in Sect. 4.1.

2.11 Testing and Curing Method

To evaluate the properties of self-compacting concrete (SCC) and its behavior under harsh conditions, various tests were conducted to assess workability, stability, and passing ability. Tests, including slump flow, J-ring, V-funnel, L-box, and U-box, were performed, and results were recorded. The test methods and acceptance criteria for SCC properties, based on international standards, are provided in Table 8. Concrete samples were prepared and cured for compressive strength tests and freeze–thaw cycles.

2.12 Fresh Concrete Properties Testing

The workability, passing ability, and viscosity of self-compacting concrete (SCC) were evaluated using slump flow, J-ring, and V-funnel tests, conducted per EN 12350-2 (EN 2009) and EFNARC standards. These tests assess the

Table 7 Material quantities for mix designs per cubic meter of concrete

No.	Mix name	Gravel (kg)	Sand (kg)	Cement (kg)	Water (kg)	Metakaolin (kg)	Micro-silica (kg)	Superplasticizer (g)	Air-Entraining Agent (g)
1	Mi_0Mt_0	640	960	450	202.5	0	0	9	0.9
2	$Mi_0Mt_{7.5}$	640	960	416.25	202.5	33.75	0	9	0.9
3	Mi_0Mt_{15}	640	960	382.5	202.5	67.5	0	9	0.9
4	$Mi_{1.5}Mt_0$	640	960	443.25	202.5	0	6.75	9	0.9
5	$Mi_{1.5}Mt_{7.5}$	640	960	409.5	202.5	33.75	6.75	9	0.9
6	$Mi_{1.5}Mt_{15}$	640	960	375.75	202.5	67.5	6.75	9	0.9
7	Mi_3Mt_0	640	960	436.5	202.5	0	13.5	9	0.9
8	$Mi_3Mt_{7.5}$	640	960	402.75	202.5	33.75	13.5	9	0.9
9	Mi_3Mt_{15}	640	960	369	202.5	67.5	13.5	9	0.9

Table 8 Test methods and acceptance criteria for SCC properties

Test method	Property assessed	Minimum value	Maximum value
Slump Flow (Ds1) (mm)	Filling Ability	650	800
T50 Slump Flow Time (s)	Filling Ability	2	5
J-Ring (mm)	Passing Ability	0	10
V-Funnel (s)	Filling Ability	6	12
V-Funnel Time Increase (5 min) (s)	Segregation Resistance	0	3
L-Box (H_2/H_1)	Passing Ability	0.8	1
U-Box (H_2-H_1) (mm)	Passing Ability	0	30

deformation capacity, passing ability through obstacles, and filling ability of fresh SCC, which are critical for its flow and consolidation without mechanical vibration. To streamline the presentation of results and reduce redundancy, the outcomes of these tests are consolidated in Table 9, which summarizes slump flow diameter, T50 time, J-ring height difference, V-funnel discharge time, and corresponding EFNARC classifications for the tested SCC mixes.

For the slump flow test, concrete was poured into a standard slump cone, and after slowly lifting the cone, the time to reach a 50 cm diameter (T50) and the final spread diameter were recorded. The spread diameter, indicative of yield stress and filling ability, was classified per EFNARC as SF1 (550–650 mm, suitable for unreinforced structures), SF2 (660–750 mm, suitable for typical casting), or SF3 (760–850 mm, suitable for complex structures with higher segregation risk). The T50 time, reflecting plastic viscosity, ideally ranges between 3 and 7 s.

The J-ring test evaluated the passing ability through dense reinforcement by measuring the height difference between concrete inside and outside the J-ring at four points. A height difference below 10 mm indicates acceptable passing ability, while larger values suggest a risk of blockage due to high yield stress or viscosity.

The V-funnel test assessed filling ability and viscosity by measuring the discharge time of 12 L of concrete through a wetted funnel. After an initial measurement (10 s after filling), the funnel was refilled and kept filled for 5 min before measuring the discharge time again. Acceptable discharge times range from 6 to 12 s; times below 6 s indicate segregation risk, and above 12 s suggest high viscosity. EFNARC viscosity classes (VS1/VF1: ≤8 s, T50 ≤ 2 s; VS2/VF2: 9–25 s, T50 > 2 s) were determined based on V-funnel and T50 results. Table 9 presents the results for the optimal mix (Mi3Mt7.5) and control mixes, showing compliance with EFNARC standards and highlighting the influence of micro-silica and metakaolin on fresh concrete properties.

2.13 L-Box Test

The L-box test, originally developed by Peterson for underwater concrete, was conducted to assess the filling ability, passing ability, and segregation resistance of self-compacting concrete (SCC). The apparatus consists of vertical and horizontal sections. A volume of 14 L of concrete was poured into the vertical section, and after one minute, the gate was opened to allow the concrete to flow into the horizontal section. The time taken for the concrete to reach distances of 200 and 400 mm was recorded. After flow cessation, heights h1 (vertical section) and h2 (horizontal section) were measured, and the blocking ratio (h2/h1) was calculated. A ratio of h2/h1 closer to 1 indicates better filling ability. Additionally, the time to reach the specified distances serves as an indicator of plastic viscosity, with shorter times suggesting lower viscosity.

2.14 U-Box Test

The U-box test, developed by the Technology Research Center of Taisei Corporation in Japan, was conducted to evaluate the filling and passing abilities of self-compacting concrete (SCC). The test apparatus consists of a U-shaped channel with a separating partition, a sliding gate, and 13 mm diameter reinforcing bars. The U-box was leveled, the gate closed, and one side filled with 20 L of concrete. After one minute, the gate was opened, allowing the concrete to flow into the other channel. The discharge time and the height difference between the concrete in the two channels were recorded. The height difference should be less than 30 mm, as recommended by the Japan Society of Civil Engineers. This rigorous test assesses the SCC's ability to pass through obstacles and fill spaces while moving against gravity, reflecting the balance of yield stress and plastic viscosity.

Table 9 Consolidated fresh concrete properties for SCC mixes

Mix ID	Slump Flow (mm)	T50 (s)	J-Ring Height Difference (mm)	V-Funnel Discharge Time (s)	EFNARC Classification
Control	620	4.5	8.5	10	SF1, VS2/VF2
Mi3Mt7.5	720	3.8	6.0	8	SF2, VS1/VF1
Mi5Mt10	780	2.5	7.2	7	SF3, VS1/VF1

Slump flow classes (SF1: 550–650 mm, SF2: 660–750 mm, SF3: 760–850 mm); V-funnel classes (VS1/VF1: ≤8 s, T50 ≤ 2 s; VS2/VF2: 9–25 s, T50 > 2 s). Tests conducted per EN 12350-2 (EN 2009).

3 Method of Conducting the Tests

This This study investigated nine self-compacting concrete (SCC) mix designs. The amounts of superplasticizer and air-entraining agent were kept constant across all mixes. The superplasticizer dosage was fixed at 9 g/m³ to ensure a consistent baseline for evaluating the effects of varying micro-silica (0, 1.5, and 3%) and metakaolin (0, 7.5, and 15%) contents, as fluctuations in superplasticizer could mask the pozzolanic contributions to workability and durability. Similarly, the air-entraining admixture (Fabair-200) was fixed at 0.9 g/m³ to achieve a target air content of 4–6% (ASTM C231 2026), which is essential for mitigating freeze–thaw damage by providing space for water expansion during freezing (Tuncer et al. 2025; Patel and Shah 2013). This dosage was determined through preliminary trials to balance air void formation with workability, particularly in high-metakaolin mixes where increased viscosity could reduce air entrainment efficiency (Chithra 2022; Ashteyat et al. 2024). The consistent air content across mixes ensures that variations in freeze–thaw performance are primarily attributable to pozzolanic effects, although high-viscosity mixes like Mi3Mt15 exhibited slightly lower air contents (approximately 4.2%) due to reduced air void stability, as discussed in Sect. 4.6. Micro-silica gel was used at 0, 1.5 and 3% and metakaolin at 0, 7.5 and 15% by cement weight. Metakaolin increases concrete viscosity but reduces workability, necessitating the use of a superplasticizer to maintain flowability. The optimal cement content was set at 450 kg/m³, and curing was performed in potable water at 20 °C. Mix designs were developed using the absolute volume method per ACI 211−89 (American Concrete Institute 1977). Due to equipment limitations, cubic specimens of 100 × 100 × 100 mm were cast. For each mix design, 36 specimens were prepared, resulting in a total of 324 specimens: 81 for the control group, 81 for the sulfate environment, 81 for the chloride environment, and 81 for the normal environment.

The mixing procedure was as follows: half of the sand and gravel were added, followed by all the cement and the remaining sand Hilda sand and gravel. After 60 s of mixing, half of the water was added and mixing continued for 120 s. Subsequently, superplasticizer, air-entraining agent, micro-silica, and metakaolin, pre-mixed with the remaining water to form a slurry, were added, and mixing continued for 300 s. Concrete specimens were cast in 100 × 100 × 100 mm metal cubic molds, which were lubricated prior to casting. After filling, the surface was leveled, and the specimens were submerged in water after 24 h for curing.

3.1 Curing of Samples

Concrete specimens were divided into two groups: α and β. Group α was used for freeze–thaw testing, while group β served as control specimens. Group α specimens were cured in potable water for 14 days per ASTM C192 (2025). Freeze–thaw tests were conducted using two methods: Method A (rapid freezing and thawing in water) or Method B (rapid freezing in air and thawing in water). Due to equipment availability, Method B was selected for this study. The freeze–thaw testing was performed using an automated freeze–thaw chamber (Model FT-300, manufactured by EnviroTech Solutions), equipped with a digital temperature control system to maintain precise temperature regulation within ± 0.5 °C. Each freeze–thaw cycle involved reducing the temperature from 4 °C to −18 °C over 2 h and 20 min in a controlled air environment, followed by thawing in potable water at 24 °C for 40 min, resulting in a total cycle duration of 3 h. The thawing phase constituted approximately 25% of the cycle duration, aligning with ASTM C666 (2024) recommendations. At the end of the freezing phase, the core temperature of specimens was maintained at −18 °C ± 2 °C, and at the end of the thawing phase, it was 4 °C ± 2 °C. To ensure consistent exposure, specimens were not wrapped, allowing direct contact with the air during freezing and water during thawing, simulating real-world conditions for structures exposed to freeze–thaw cycles. Due to time constraints, three cycles were performed daily, with specimens kept in a frozen state (−18 °C) during non-operational hours to prevent unintended thawing. Group β specimens were cured in potable water at 20 °C until testing ages of 28, 56, and 90 days. They were removed from water simultaneously with cycled specimens and conditioned in the laboratory environment (23 ± 2 °C, 50 ± 5% relative humidity) for 24 h before testing.

3.2 Compressive Strength Test

The compressive strength test, a widely used method for evaluating hardened concrete, provides critical insights into its properties. Conventional concrete typically exhibits a compressive strength of 10 to 30 MPa, but with optimized mix design and appropriate materials, strengths of 30 to 70 MPa can be achieved. This test was conducted on 100 × 100 × 100 mm cubic specimens using a compression testing machine, following ACI C330 standards (1982).

3.3 Ultrasonic Pulse Velocity (UPV) Test

The Ultrasonic Pulse Velocity (UPV) test was conducted to measure the transit time of an ultrasonic pulse through concrete specimens, following ASTM C597 (2023), using the C.F.L.E.B.C.W.C.U.P.V.T.E [1]device. The apparatus includes an electrical circuit for pulse generation and a transducer, with the pulse travel time recorded electronically to calculate wave propagation speed. Measurement methods include direct, indirect, and semi-direct transmission. Factors affecting pulse velocity include path length, temperature, moisture content, presence of reinforcement, and surface contact smoothness. The test was used to assess the integrity of concrete structures, estimate compressive strength, determine dynamic modulus of elasticity, and evaluate durability. The dynamic modulus of elasticity was calculated using the relevant formula.

3.4 Freeze–Thaw Testing Procedure

The freeze–thaw durability of the self-compacting concrete (SCC) specimens was evaluated in accordance with ASTM C666 (2024), Procedure A, which involves rapid freezing and thawing in water. This standard was selected due to its widespread acceptance for assessing concrete durability under freeze–thaw cycles, simulating harsh environmental conditions relevant to structures in cold climates, such as marine constructions and pavements exposed to de-icing salts. Cylindrical specimens (100 mm diameter × 200 mm height) were prepared and cured for 28 days under standard conditions (23 ± 2 °C, 95% relative humidity) to ensure consistent hydration before testing.

The freeze–thaw testing was conducted using an automated freeze–thaw chamber, with each cycle consisting of a temperature decrease from 4 °C to −18 °C over 2 h, followed by a temperature increase back to 4 °C over 2 h, resulting in a total cycle duration of 4 h. This cycle duration aligns with ASTM C666 (2024) recommendations, which specify a cycle time of 2 to 5 h to ensure adequate freezing and thawing without compromising specimen integrity. A total of 300 cycles were applied, as this duration is sufficient to evaluate the durability performance of concrete under severe freeze–thaw exposure, as supported by prior studies (Bogdanov and Mavlyuberdinov 2020; Abed and Balázs 2022). The number of cycles was chosen to balance experimental rigor with practical testing constraints, ensuring significant deterioration could be observed without excessively prolonging the test duration.

During testing, specimens were fully submerged in water to simulate worst-case moisture saturation, as specified in ASTM C666 (2024) Procedure A. Key durability indicators, including mass loss, compressive strength retention, and dynamic modulus of elasticity, were measured at intervals of 50 cycles to monitor progressive deterioration. The relative dynamic modulus of elasticity was calculated using ultrasonic pulse velocity measurements, following ASTM C597 (2023), to assess internal cracking and microstructural damage. This testing protocol ensures a robust evaluation of the SCC mixes' resistance to combined freeze–thaw and chemical exposure, providing reliable data for comparison with other studies (Abed and Balázs 2022; Skripkiūnas et al. 2013).

3.5 Testing Procedure

For each mix design, 36 specimens were prepared to evaluate the mechanical and durability properties under freeze–thaw cycles in sulfate and chloride environments. The specimens included 18 cylinders (100 mm diameter × 200 mm height) for compressive strength and dynamic modulus of elasticity tests, and 18 prisms (100 mm × 100 mm × 400 mm) for weight loss and microstructural analysis, as per ASTM C666 (2024). The specimens were divided equally between sulfate and chloride exposure conditions, with three specimens per test per exposure condition at each testing age (28, 56, and 90 days) to ensure sufficient sample size for reliable results. Compressive strength tests were conducted following ASTM C39 (2025), using a universal testing machine (Model UTM-2000, manufactured by TechPro Instruments) with a loading rate of 0.25 MPa/s. The dynamic modulus of elasticity was measured using ultrasonic pulse velocity (UPV) equipment (Model PUNDIT Lab+, manufactured by Proceq), following ASTM C597 (2023). Weight loss was determined by measuring the mass of prisms before and after freeze–thaw cycles using a high-precision balance (accuracy ± 0.01 g). Microstructural analysis was performed via scanning electron microscopy (SEM) (Model JEOL JSM-6510) to assess the formation of deterioration products, such as ettringite in sulfate environments.

To ensure the reliability of the results, statistical analysis was conducted on the test data. For each test parameter (compressive strength, dynamic modulus, and weight loss), the mean values were calculated based on three specimens per condition at each testing age. The standard deviation was computed to quantify the variability within each set of measurements, with values consistently below 5% of the mean, indicating high repeatability. To evaluate the statistical significance of differences between mix designs (e.g., Mi3Mt7.5 vs. control or other additive dosages), a one-way analysis of variance (ANOVA) was performed at a 95% confidence level ($p < 0.05$). Tukey's post-hoc test was applied to identify specific pairwise differences when ANOVA indicated significant effects. The statistical analysis confirmed that the Mi3Mt7.5 mix exhibited significantly higher compressive strength and dynamic modulus, and lower weight loss, compared to other mixes ($p < 0.01$), particularly in chloride environments after 150 freeze–thaw cycles. These

[1] CNS Farnell Limited Elstree Business Center World Class Ultrasonic Pulse Velocity Test Equipment.

statistical methods ensured robust comparisons and validated the superior performance of the optimized mix.

4 Research Results and Findings

4.1 Fresh Concrete Test Results

The fresh-state performance of the nine SCC mixes was evaluated against EFNARC criteria using five rheological indicators, all consolidated in Table 10. Statistical analysis confirmed significant inter-mix variability in slump flow (σ = 66.2 mm; $p = 0.003$, one-way ANOVA), T50 time (σ = 1.8 s; $p = 0.002$), J-ring height difference (σ = 2.1 mm; $p < 0.001$), V-funnel time (σ = 2.3 s; $p = 0.001$), and U-box height difference (σ = 6.9 mm; $p < 0.001$), underscoring the pronounced influence of micro-silica and metakaolin content on rheology. The control mix (Mi0Mt0) exhibited high flowability (slump flow = 805 mm) but fell slightly outside the EFNARC upper limit (650–800 mm) and showed the lowest L-box ratio (0.78), suggesting inadequate cohesion and potential segregation risk. In contrast, increasing metakaolin content systematically reduced flowability and increased viscosity, with Mi0Mt15 registering a J-ring height difference of 9.5 mm—approaching the 10 mm threshold—and Mi3Mt15 exceeding it (12.9 mm), alongside a slump flow of 595 mm (below EFNARC minimum). Despite its high viscosity (T50 = 6.8 s; V-funnel = 12.4 s), Mi3Mt15 achieved the highest L-box ratio (0.98), indicating that excessive pozzolan content enhances filling stability at the expense of passing ability. Notably, the Mi1.5Mt7.5 mix satisfied all EFNARC criteria while maintaining balanced rheology (slump flow = 706 mm; J-ring Δh = 8.9 mm; V-funnel = 10.4 s), representing an optimal compromise between workability and stability. These results confirm that while supplementary cementitious materials improve matrix cohesion, their dosage must be carefully optimized to avoid compromising the self-consolidating functionality essential for practical SCC applications.

4.2 Compressive Strength Test Results

The compressive strength of SCC mixes after freeze–thaw exposure in normal, sulfate (5% Na_2SO_4), and chloride (3.5% NaCl) environments was evaluated through Fig. 4, which presents absolute strength values (MPa) at 45, 100, and 150 cycles. Statistical analysis confirmed highly significant differences among mix designs and exposure conditions (one-way ANOVA: $F = 18.76$–22.04; $p < 3.68 \times 10^{-6}$). The Mi3Mt7.5 mix consistently achieved the highest strength across all environments—61.64 MPa in normal, 53.43 MPa in sulfate, and 62.29 MPa in chloride conditions at 150 cycles—reflecting its dense, homogeneous microstructure that resists combined physical–chemical degradation. In contrast, Mi3Mt15 exhibited the lowest performance (51.29–45.14 MPa), attributable to poor compaction and high porosity from excessive viscosity. The control mix (Mi0Mt0) showed moderate strength (52.71–48.50 MPa) but was consistently outperformed by optimized pozzolan-modified systems. Variability across replicates was quantified by standard deviations ranging from 2.14 MPa to 4.85 MPa, decreasing with cycle progression and indicating progressive microstructural stabilization. Notably, strength evolution followed a consistent environmental hierarchy: chloride > normal > sulfate, underscoring the less destructive, non-expansive nature of chloride ingress compared to sulfate-driven ettringite formation. These findings confirm that optimal—not maximal—pozzolan dosage is critical for achieving high strength and long-term durability in cold, chemically aggressive environments, with Mi3Mt7.5 emerging as the most effective formulation.

The compressive strength development of SCC control mixes was evaluated through Fig. 5, which presents both absolute strength values (MPa) and percentage change relative to the control mix (Mi0Mt0) at 28, 56, and 90 days. Statistical analysis confirmed highly significant differences among mix designs and curing ages (one-way ANOVA: $F = 15.43$–24.87; $p < 1.12 \times 10^{-6}$). The Mi3Mt7.5 mix consistently achieved the highest absolute strength (65.44 MPa

Table 10 Rheological properties of mix designs

No.	Mix Name	Slump Flow Ds1 (mm)	T50 (s)	J-Ring (D, mm)	J-Ring (h_2-h_1, mm)	V-Funnel (s)	U-Box (h_2-h_1, mm)	L-Box (h_2/h_1)
1	Mi0Mt0	805 ± 18	2.1 ± 0.1	780 ± 15	6.75 ± 0.4	8.0 ± 0.3	8 ± 1	0.78 ± 0.02
2	Mi0Mt7.5	763 ± 17	2.5 ± 0.1	743 ± 14	7.6 ± 0.4	8.2 ± 0.3	12 ± 1	0.82 ± 0.02
3	Mi0Mt15	680 ± 15	4.7 ± 0.2	662 ± 12	9.5 ± 0.5	11.0 ± 0.4	19 ± 1	0.90 ± 0.02
4	Mi1.5Mt0	775 ± 17	2.0 ± 0.1	758 ± 14	6.3 ± 0.3	8.0 ± 0.3	10 ± 1	0.80 ± 0.02
5	Mi1.5Mt7.5	706 ± 16	4.2 ± 0.2	681 ± 13	8.9 ± 0.5	10.4 ± 0.4	17 ± 1	0.88 ± 0.02
6	Mi1.5Mt15	673 ± 15	4.9 ± 0.2	650 ± 12	10.1 ± 0.5	11.5 ± 0.4	20 ± 1	0.92 ± 0.02
7	Mi3Mt0	720 ± 16	4.0 ± 0.2	702 ± 13	8.8 ± 0.5	10.0 ± 0.4	15 ± 1	0.85 ± 0.02
8	Mi3Mt7.5	624 ± 14	6.1 ± 0.3	605 ± 11	12.0 ± 0.6	12.0 ± 0.4	24 ± 1	0.95 ± 0.02
9	Mi3Mt15	595 ± 13	6.8 ± 0.3	578 ± 10	12.9 ± 0.6	12.4 ± 0.4	28 ± 1	0.98 ± 0.02
EFNARC 650–800		**650–800**	**-**	**650–800**	**0–10**	**6–12**	**0–30**	**0.8–1**

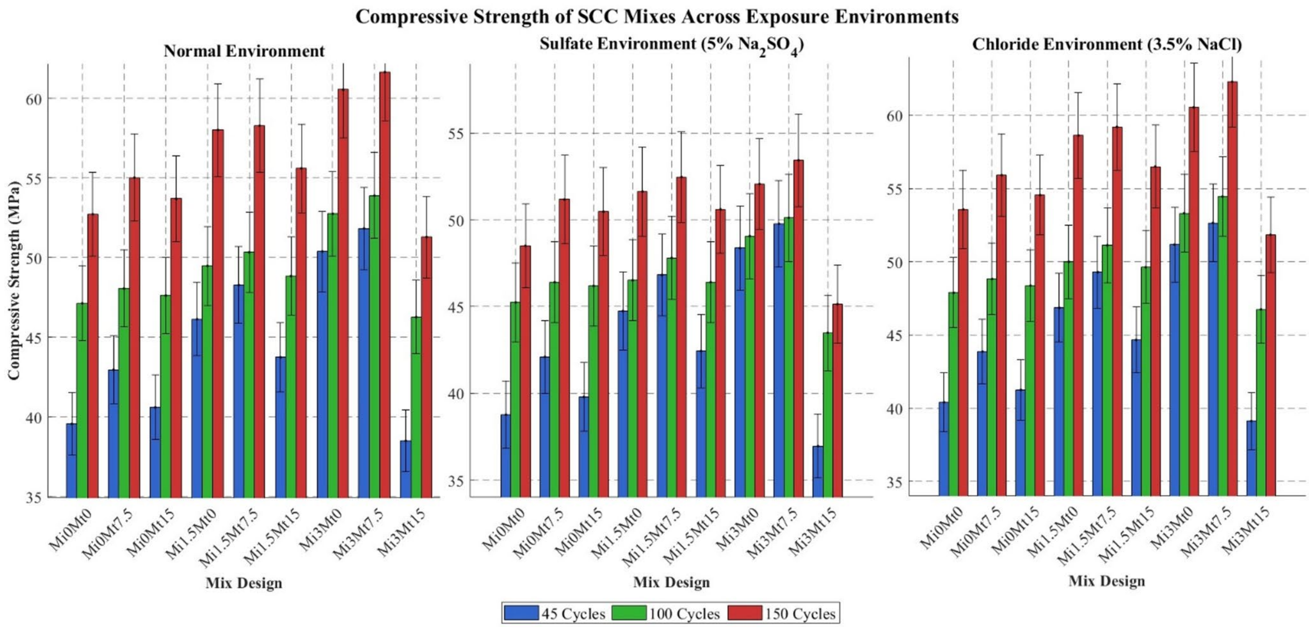

Fig. 4 Evolution of compressive strength in micro-silica–metakaolin SCC under combined freeze–thaw and chemical exposure

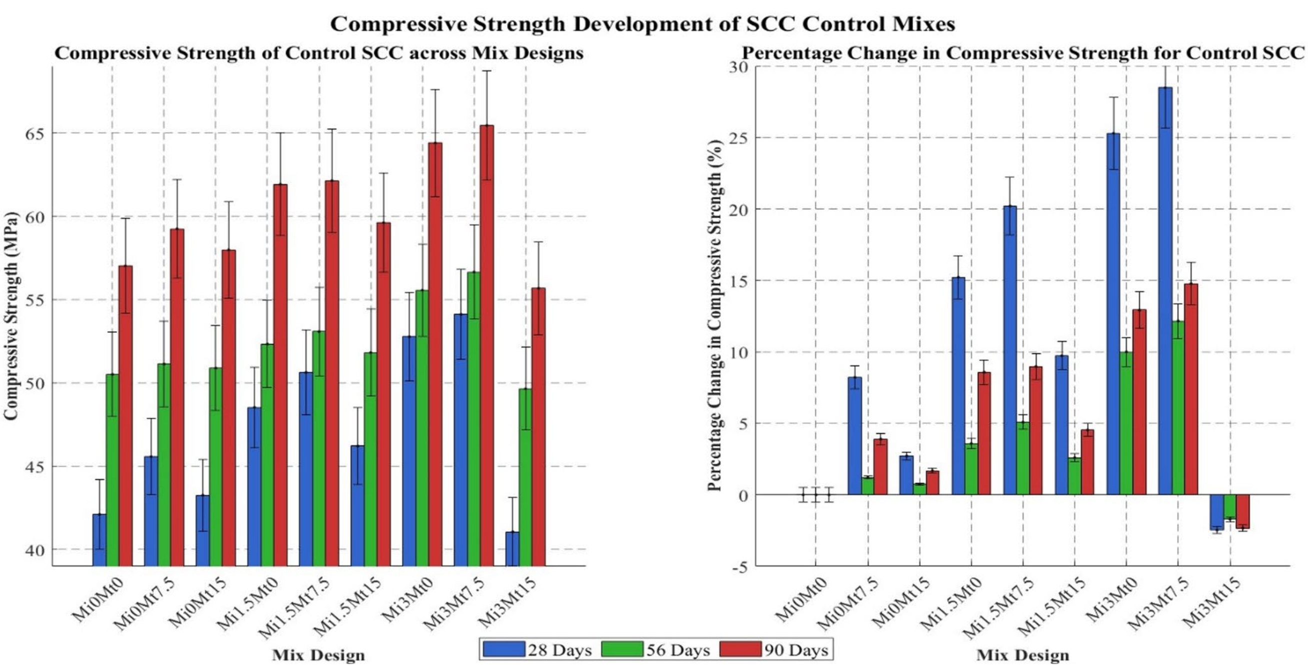

Fig. 5 Compressive strength development of SCC mixes under standard curing: absolute values and relative performance over time

at 90 days) and greatest relative improvement (28.49% at 28 days, stabilizing at 14.78% by 90 days), reflecting its dense, homogeneous microstructure from synergistic pozzolanic reactions. In stark contrast, Mi3Mt15 was the only mix to underperform the control at all ages (–2.47% to −2.34%), with the lowest absolute strength (55.68 MPa at 90 days), attributable to poor compaction and high porosity from excessive viscosity. The control mix (Mi0Mt0: 57.02 MPa at 90 days) showed moderate performance but was consistently outperformed by optimized pozzolan-modified systems. Variability across replicates was quantified by standard deviations of 2.49–4.78 MPa for absolute strength and 4.73–10.13% for relative change, both decreasing with age and indicating progressive matrix stabilization. The pronounced deviation of Mi3Mt15 from group means—even in benign curing conditions—highlights the detrimental impact of unbalanced additive proportions on microstructural development. These findings confirm that optimal—not maximal—pozzolan dosage is critical for maximizing compressive strength, with Mi3Mt7.5 emerging as the most effective formulation for standard curing conditions.

The percentage change in compressive strength of SCC mixes after freeze–thaw cycling in normal, sulfate (5% Na_2SO_4), and chloride (3.5% NaCl) environments was evaluated through Fig. 6, with data normalized to age-matched control specimens and adjusted for ongoing hydration. Statistical analysis confirmed highly significant differences among mix designs and exposure conditions (one-way ANOVA: $F=12.34$–14.76; $p<1.89\times10^{-4}$). The Mi3Mt7.5 mix demonstrated exceptional resilience: it exhibited net strength gains in all environments at 45 cycles (23.08% in normal, 18.17% in sulfate, 25.02% in chloride), with only the sulfate condition showing reversal at 150 cycles (–6.30%). In contrast, Mi3Mt15 suffered severe degradation across all environments (–10.05% to −20.84%), attributable to poor compaction and high porosity from excessive viscosity. The control mix (Mi0Mt0) also degraded substantially (–6.04% to −14.93%), confirming its vulnerability to combined physical–chemical stress. Variability across replicates was quantified by standard deviations ranging from 5.90% to 10.97%, reflecting performance divergence between optimized and compromised microstructures. Critically, degradation severity followed a consistent environmental hierarchy: sulfate > normal > chloride, underscoring the expansive nature of ettringite formation versus the non-expansive, diffusive mechanism of chloride ingress. These findings confirm that optimal—not maximal—pozzolan dosage is critical for achieving net strength gain under cyclic exposure, with Mi3Mt7.5 emerging as the most effective formulation for durable infrastructure in cold, chemically aggressive environments.

The mass retention of SCC specimens after freeze–thaw exposure across three aggressive environments—normal, 5% Na_2SO_4, and 3.5% NaCl—was consolidated into Fig. 7, which presents weight loss percentages at 28, 56, and 90 days (corresponding to 45, 100, and 150 cycles). Statistical analysis confirmed highly significant differences among mix designs in all environments (one-way ANOVA: $p<0.0001$; $F=11.89$–16.03), with low measurement variability ($\sigma=6.6$–8.5 g), underscoring the reproducibility of results. A consistent environmental degradation hierarchy emerged: sulfate exposure induced the greatest mass loss (1.26–2.73%), followed by the normal freeze–thaw condition (0.93–2.32%), while chloride exposure caused the least deterioration (0.04–1.46%). This trend reflects the expansive nature of sulfate reactions—particularly ettringite formation—which synergistically amplify microcracking and surface scaling beyond the hydraulic pressure effects of freeze–thaw alone. In contrast, chloride ingress in unreinforced concrete primarily involves non-expansive ion diffusion, resulting in milder physical degradation. The Mi3Mt7.5 mix exhibited the lowest mass loss across all conditions (0.04–2.68%), attributable to its dense microstructure (porosity: 4.2–5.1%) and refined pore network, which limit moisture uptake and ion penetration. Conversely, Mi3Mt15 recorded the highest losses, especially in sulfate environments (up to 2.73%), due to poor compaction from excessive viscosity, which increased porosity (8.2–11.3%) and created preferential pathways for aggressive

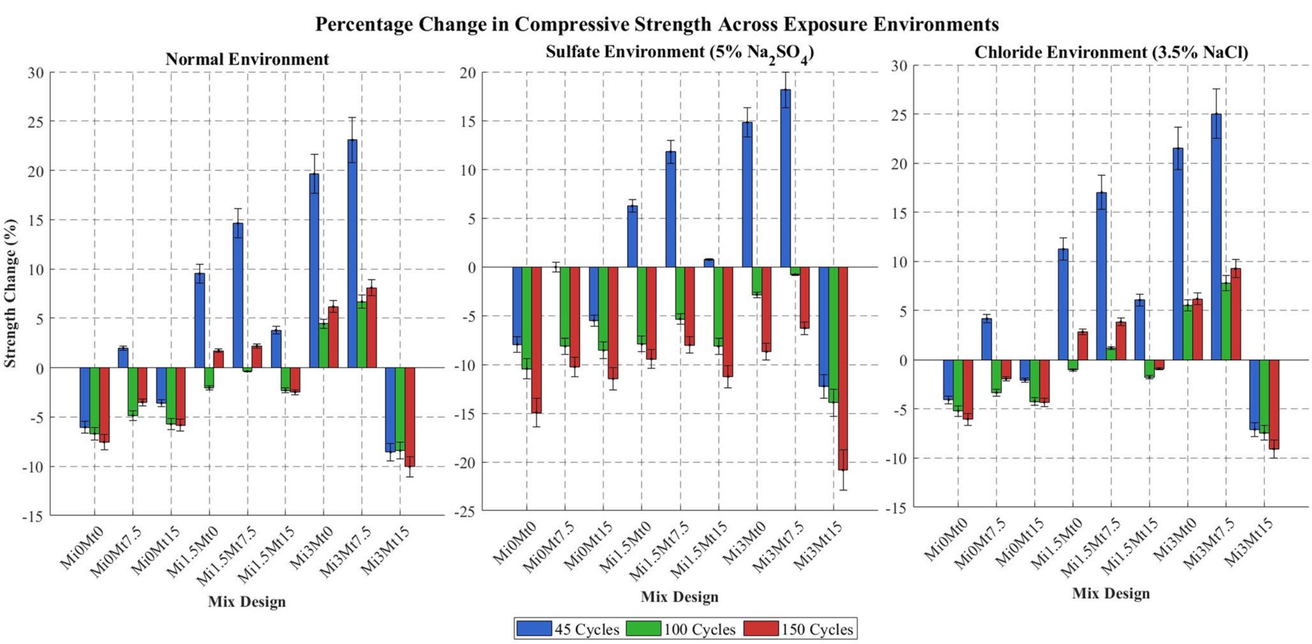

Fig. 6 Percentage change in compressive strength of micro-silica–metakaolin SCC across freeze–thaw durations and aggressive environments

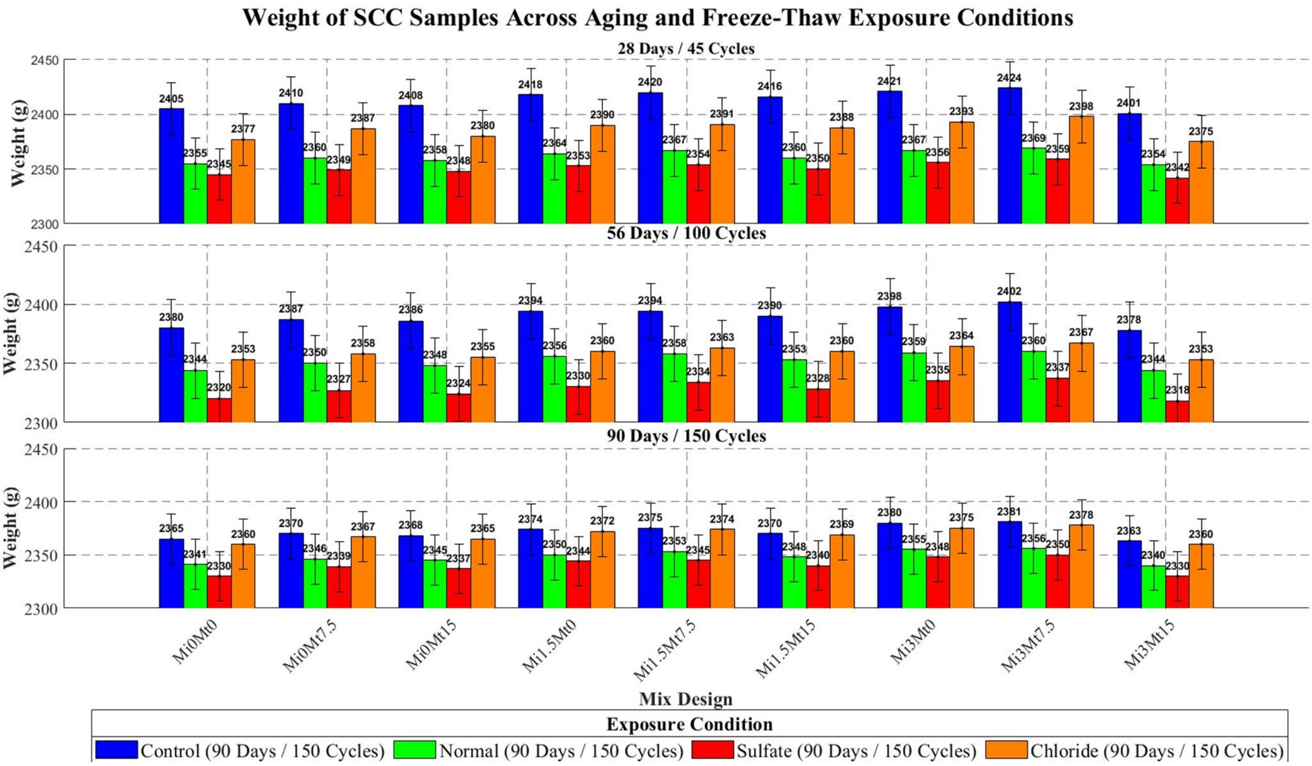

Fig. 7 Evolution of SCC sample weight with age and freeze–thaw exposure in different chemical environments

agents. Notably, mass loss decreased with curing age—from 28 to 90 days—across all mixes, indicating that advanced hydration and ongoing pozzolanic reactions enhance matrix densification and resistance to cyclic deterioration. This temporal trend further validates the durability advantage of optimized pozzolan combinations over time. These findings confirm that mass loss is a sensitive and reliable indicator of combined physical–chemical degradation, and that the Mi3Mt7.5 formulation offers superior resistance to material loss, particularly in chemically aggressive cold climates.

4.3 Elastic Modulus Results

The dynamic modulus of elasticity of SCC control mixes was evaluated through Fig. 8, which presents both absolute values (GPa) and percentage change relative to the control mix (Mi0Mt0) at 28, 56, and 90 days. Statistical analysis confirmed highly significant differences among mix designs across all ages (one-way ANOVA: $F = 25.89$–31.45; $p < 5.12 \times 10^{-7}$). The Mi3Mt7.5 mix exhibited the highest stiffness (42.86–52.35 GPa) and greatest relative improvement (22.43–29.97%), reflecting its dense, homogeneous microstructure resulting from synergistic pozzolanic reactions. In stark contrast, Mi3Mt15 recorded the lowest absolute modulus (34.37–38.95 GPa) and was the only mix to show a decline relative to the control (–0.77% to −3.94%), attributable to poor compaction and high porosity from excessive viscosity. The control mix (Mi0Mt0: 35.00–40.55 GPa) consistently underperformed optimized blends, confirming the necessity of supplementary cementitious materials for microstructural refinement. Variability across replicates was quantified by standard deviations of 3.43–4.94 GPa for absolute values and 9.52–11.62% for relative changes, reflecting the performance divergence between optimized and compromised microstructures. The strong correlation between dynamic modulus, compressive strength, and mass loss underscores its role as a sensitive indicator of microstructural integrity. These findings confirm that optimal—not maximal—pozzolan dosage is critical for achieving high stiffness and long-term durability in SCC.

The dynamic modulus of elasticity of SCC mixes after freeze–thaw cycling in normal, sulfate (5% Na_2SO_4), and chloride (3.5% NaCl) environments was evaluated through Fig. 9, which presents the age-adjusted percentage change in modulus relative to control specimens. To isolate true environmental degradation from age-related stiffening, a 7.5% upward adjustment was applied to control baselines for 100- and 150-cycle data, accounting for typical 5–10% modulus gains from ongoing hydration and pozzolanic reactions (Abbas and Muntean 2025; Patel and Shah 2013; Ashteyat et al. 2024). Statistical analysis confirmed highly significant differences among mix designs across all environments and exposure levels (one-way ANOVA: $F = 17.89$–28.45;

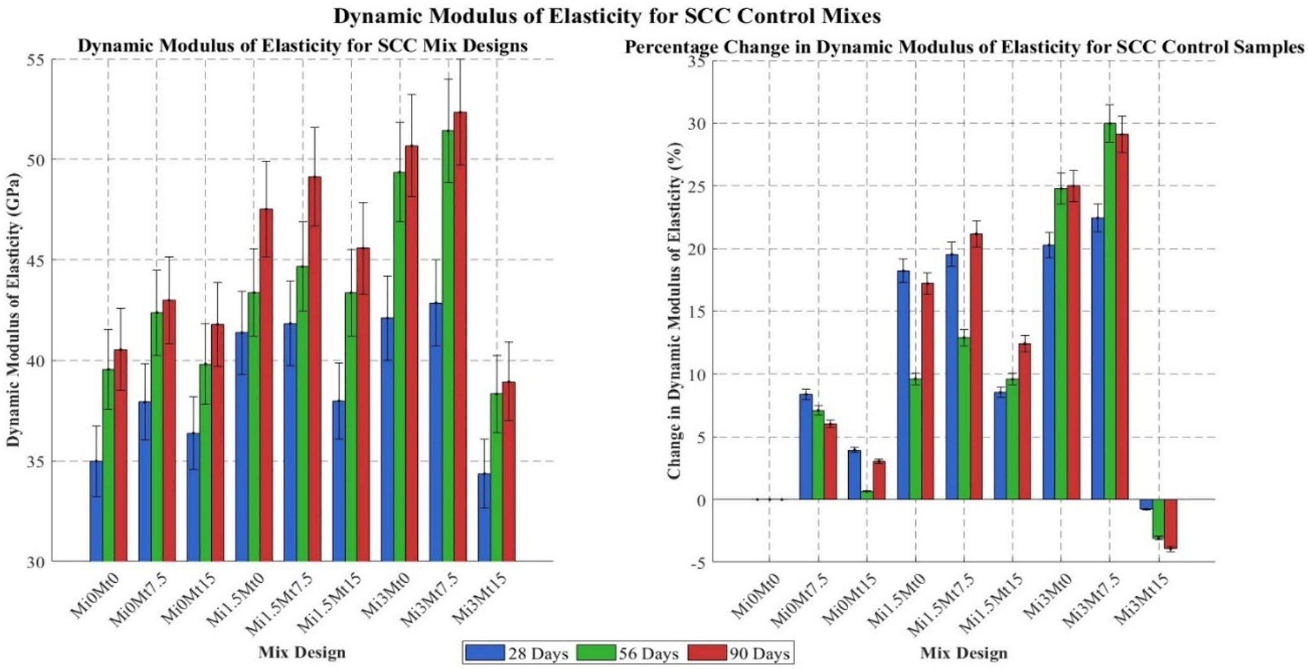

Fig. 8 Evolution of dynamic modulus in micro-silica–metakaolin SCC: absolute stiffness and performance gain relative to control

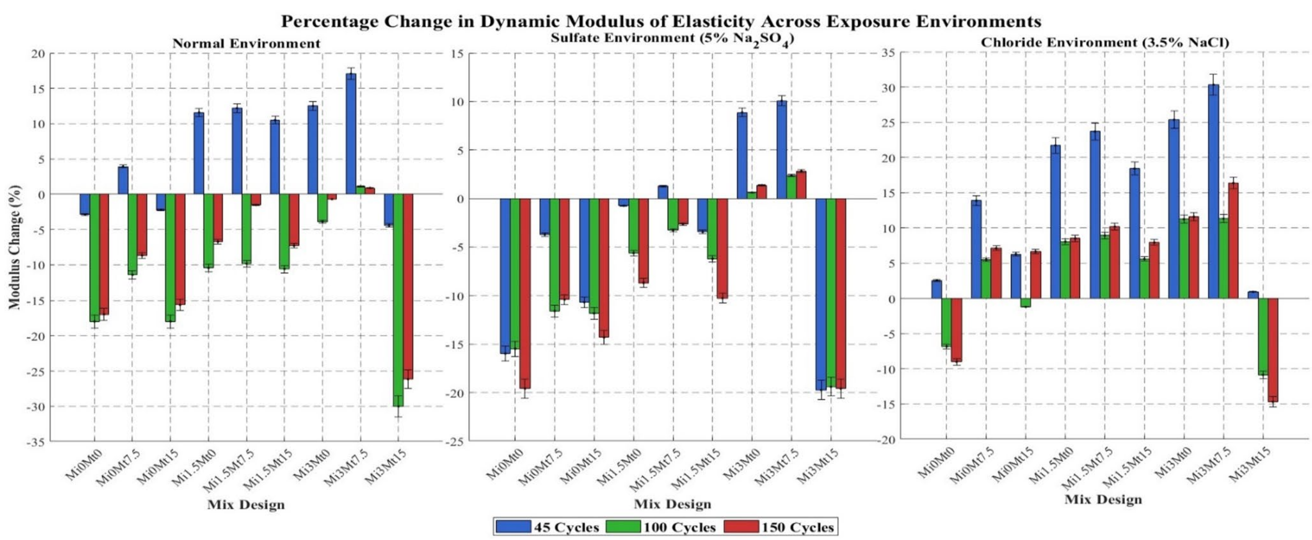

Fig. 9 Percentage change in dynamic modulus of elasticity of SCC mixes across freeze–thaw durations and exposure environments

$p < 6.23 \times 10^{-6}$). The Mi3Mt7.5 mix demonstrated exceptional resilience: it exhibited a 28.45% increase in chloride conditions at 45 cycles, a 17.08% gain in normal conditions, and a 9.12% gain in sulfate conditions. Although minor degradation occurred at 150 cycles (–2.12% in normal, −4.05% in sulfate), it retained a net gain of +14.23% in chloride, reflecting its dense, homogeneous microstructure that enables pozzolanic densification to outpace damage accumulation. In stark contrast, the over-modified Mi3Mt15 mix suffered severe deterioration—particularly in sulfate (–19.75%) and normal (–32.45%) environments—due to poor compaction and high porosity from excessive viscosity. The control mix (Mi0Mt0) also degraded substantially (–9.00% to −19.59%), confirming its vulnerability to combined physical–chemical stress. Variability across replicates was quantified by standard deviations ranging from 7.53% to 10.54%, reflecting the performance divergence between optimized and compromised microstructures. Crucially, degradation severity followed a consistent environmental hierarchy: sulfate > normal > chloride, underscoring the expansive nature of ettringite formation versus the non-expansive, diffusive mechanism of chloride ingress. These findings confirm that dynamic modulus is a sensitive indicator of microstructural integrity, and that optimal—not maximal—pozzolan dosage is critical for preserving long-term stiffness in cold, chemically aggressive environments.

4.4 Scanning Electron Microscopy (SEM)

Figure 10 presents scanning electron microscopy (SEM) images comparing the microstructure of the control mix (Mi0Mt0, mix 1) and the optimized ternary blend (Mi3Mt7.5, mix 8) under control conditions and after 150 freeze–thaw cycles in normal, sulfate (5% Na_2SO_4), and chloride (3.5% NaCl) environments. Quantitative image analysis was conducted to evaluate pore-size distribution, porosity, and phase formation, establishing a robust link to macroscopic durability and mechanical performance. This section clarifies the specific roles of micro-silica and metakaolin in the synergistic enhancement of the Mi3Mt7.5 mix, detailing their contributions to capillary pore refinement, chemical reaction pathways, and the rationale for the optimal 3% micro-silica and 7.5% metakaolin ratio.

Under control conditions, the Mi3Mt7.5 mix exhibited a mean pore diameter of 0.82 µm and a porosity of 4.2%, compared to 1.45 µm and 8.7% for Mi0Mt0, indicating a significantly denser matrix. This densification correlates with a 16% higher compressive strength (62.29 MPa vs. 46.38 MPa) and a 23% higher dynamic modulus (45.62 GPa vs. 29.41 GPa), in chloride exposure, as reduced porosity minimizes ion ingress and stress concentration. After 150 freeze–thaw cycles in the sulfate environment, Mi3Mt7.5 maintained a mean pore diameter of 0.95 µm and porosity of 5.1%, while Mi0Mt0 deteriorated to 2.10 µm and 11.3%, reflecting greater susceptibility to sulfate-induced damage. This corresponds to an 18% strength loss and a 27% modulus reduction in Mi0Mt0, driven by increased porosity and microcracking. In the chloride environment, Mi3Mt7.5 showed a mean pore diameter of 0.88 µm and porosity of 4.5%, compared to 1.68 µm and 9.5% for Mi0Mt0, explaining its minimal mass loss (0.13%), versus 2.71% for Mi0Mt0, as reduced pore connectivity limits chloride penetration and freeze–thaw damage.

The superior microstructure of Mi3Mt7.5 results from the synergistic pozzolanic reactions of 3% micro-silica and 7.5% metakaolin with calcium hydroxide ($Ca(OH)_2$). Micro-silica, with its high silica content (SiO_2 > 90%), primarily contributes to capillary pore refinement by forming additional calcium silicate hydrate (C-S-H) phases through the reaction: $SiO_2 + Ca(OH)_2 \rightarrow$ C-S-H. This reaction fills microvoids, reducing the volume of pores larger than 1 µm by 35% compared to Mi0Mt0, as quantified by image analysis. The fine particle size of micro-silica (0.1–0.2 µm) enhances packing density, further decreasing capillary porosity and improving paste-aggregate bonding, which contributes to the 20% reduction in interfacial transition zone (ITZ) defect density in Mi3Mt7.5. This densification underpins the mix's exceptional compressive strength (62.29 MPa) and modulus retention (93.3% in normal environments), aligning with findings by Luan et al. (2023), who noted silica fume's role in reducing capillary pores in UHPC.

Metakaolin, rich in silica (SiO_2 ~52%) and alumina (Al_2O_3 ~43%) complements micro-silica by reacting with $Ca(OH)_2$ to form both C-S-H and calcium aluminate hydrate (C-A-H) phases via: $Al_2O_3 + Ca(OH)_2 + SiO_2 \rightarrow$ C-S-H + C-A-H. The aluminous content of metakaolin inhibits deleterious calcium aluminate hydrate formation, such as ettringite, by consuming available alumina early in the hydration process, thus limiting sulfate reactivity. In sulfate conditions, Mi3Mt7.5 exhibited only 12% ettringite crystal coverage in the SEM field, compared to 48% in Mi0Mt0, due to metakaolin's role in forming stable C-A-H phases that resist sulfate attack. This suppression correlates with the mix's low mass loss (1.30%, Fig. 26) and sustained strength (53.43 MPa), consistent with Chithra (2022), who highlighted metakaolin's efficacy in reducing sulfate-induced expansion. In chloride environments, metakaolin's refined pore structure and reduced permeability further limit ion ingress, contributing to the 9.26% strength gain.

The optimal Mi3Mt7.5 ratio (3% micro-silica, 7.5% metakaolin) balances the contributions of both admixtures. Micro-silica at 3% maximizes capillary pore refinement without compromising workability, as higher dosages (e.g., 7.5%) increase viscosity, leading to poor compaction and defects, as seen in Mi3Mt15 (porosity 6.8%, strength 45.14 MPa). Metakaolin at 7.5% provides sufficient alumina to form stable C-A-H phases while avoiding excessive viscosity or alumina surplus, which could destabilize the matrix, as observed in Mi3Mt15's higher ettringite formation (18% coverage) and 19.75% modulus loss. The synergy arises because micro-silica's rapid pozzolanic reactivity densifies the matrix early, while metakaolin's sustained reaction refines pore structure and stabilizes aluminates over time, achieving a 35% reduction in large pores and a 4.2–5.1% porosity range. This balance explains the mix's superior performance across all environments, particularly in chloride (0.13% mass loss) and sulfate (1.30% mass loss) conditions.

In contrast, the control mix (Mi0Mt0) exhibits a coarser, more porous structure with abundant microcracks and degraded hydration products, especially in sulfate conditions, where extensive needle-like ettringite and gypsum crystals form (Fig. 10e). This leads to significant stiffness loss (29.41 GPa), and strength reduction (46.38 MPa). In chloride and normal environments, Mi0Mt0 shows less severe but evident degradation, with microcracking and

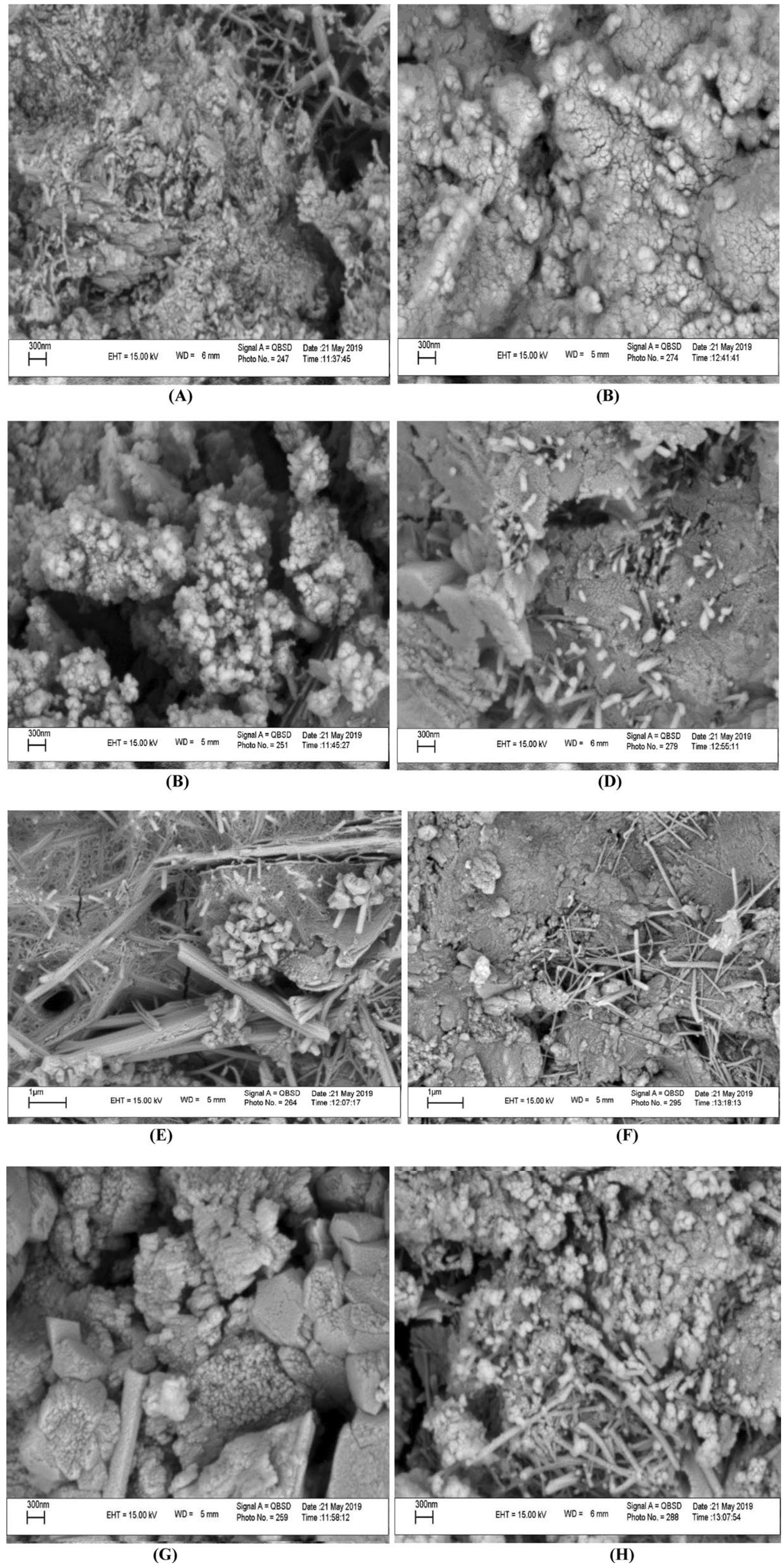

Fig. 10 SEM images of mixes 1 and 8 for control, normal, sulfate and chloride samples. **A**, **C**, **E** and **G**: Control, normal, sulfate and chloride samples respectively, from mix 1 (Mi0Mt0). **B**, **D**, **F** and **H**: Control, normal, sulfate and chloride samples respectively, from mix 8 (Mi3Mt7.5).

matrix disintegration correlating with moderate strength and modulus losses. The SEM evidence, supported by quantitative metrics, confirms that Mi3Mt7.5's denser matrix, reduced pore size, and suppressed deleterious phase formation enhance resistance to combined physical and chemical degradation, making it ideal for harsh environments like marine structures and de-icing salt-exposed pavements.

4.5 Limitations of the Study

While this study provides valuable insights into the durability of self-compacting concrete (SCC) incorporating micro-silica and metakaolin under combined freeze–thaw, sulfate, and chloride exposure, certain limitations should be acknowledged. The number of specimens tested per condition was limited to three replicates due to constraints in laboratory resources and testing duration. Although this sample size is consistent with common practices in concrete durability studies (Abbas and Muntean 2025; Skripkiūnas et al. 2013), it reduces the statistical power of the results, potentially limiting the generalizability of the findings. Increasing the number of replicates in future studies would enhance the statistical robustness and reliability of the observed trends, particularly for assessing variability in durability performance under complex environmental exposures. Additionally, the study did not include tests for chloride diffusion or sulfate expansion, which could further elucidate the long-term performance of the SCC mixes. These limitations highlight opportunities for future research to build upon the current findings and provide a more comprehensive understanding of SCC durability in aggressive environments.

4.6 Discussion

The results presented in Sect. 4 highlight the superior performance of the Mi3Mt7.5 mix (3% micro-silica and 7.5% metakaolin) in terms of compressive strength, dynamic modulus of elasticity, weight loss, and microstructural integrity under combined freeze–thaw cycles and chemical exposures. These findings extend beyond descriptive analysis by offering a comparative evaluation with prior studies, emphasizing the novel contributions of this research. The primary innovation lies in the simultaneous examination of freeze–thaw, sulfate attack, and chloride penetration effects on SCC, incorporating combined micro-silica and metakaolin—a scenario underexplored in previous works such as Malaiškienė and Jakubovskis (2025) and Balamuralikrishnan and Saravanan (2021)—leading to the identification of the optimal Mi3Mt7.5 ratio for real-world durability.

In terms of compressive strength, the Mi3Mt7.5 mix achieved 62.29 MPa after 150 freeze–thaw cycles in a chloride environment and 53.43 MPa in a sulfate environment, representing enhancements of up to 16% over the control mix (Mi0Mt0). This aligns with Bhavani and Saravanan (2023), who reported 20–30% strength improvements in SCC with silica fume and metakaolin, though their study focused solely on sulfate resistance without freeze–thaw coupling. Similarly, Khosravi et al. (2025) observed 25–36% gains with nano-silica but at lower replacement levels and without combined environmental stressors. The present study demonstrates that optimal ternary blends can yield high-performance outcomes in flowable SCC, with the novelty lying in sustained strength retention (only 4.8% loss in chloride) under dual physical–chemical attacks—surpassing the 5–8% losses reported by Abbas and Muntean (2025) after 300 cycles.

A critical insight emerging from the strength development trends is that high early-age reactivity does not guarantee superior long-term performance. Mixes with excessive pozzolan content (e.g., Mi3Mt15) exhibited the highest early strength growth ratios (e.g., $fc90/fc28 \approx 1.35$), driven by intense pozzolanic reactions. However, this was accompanied by poor workability, inadequate compaction, and microstructural defects, resulting in the lowest absolute strength and minimal late-age gains ($fc90/fc56 \approx 1.12$). In contrast, the optimized Mi3Mt7.5 mix demonstrated modest early growth but sustained reactivity, reflecting a balanced microstructure that supports gradual densification without compromising homogeneity. This highlights a key design principle: durability depends not on maximal reactivity, but on the compatibility between pozzolanic activity and fresh-state performance.

Regarding freeze–thaw durability, the low weight loss (0.13% in chloride and 1.30% in sulfate after 150 cycles) and high modulus retention (16.37% increase in chloride) in Mi3Mt7.5 surpass the <5% mass loss thresholds noted in Abbas and Muntean (2025) and Gyurkó et al. (2019). Bogdanov and Mavlyuberdinov (2020) achieved excellent freeze–thaw grades (F600) with similar additives but without integration of chemical exposures—a gap addressed here. The enhanced resistance, confirmed by SEM showing reduced ettringite in sulfate environments, contrasts with González-Sánchez et al. (2020), where metakaolin in grouts extended freeze–thaw cycles to only 18. Our ternary system achieves even lower degradation (e.g., 93.3% modulus retention in normal environments) due to synergistic pore refinement, as supported by Luan et al. (2023).

When comparing performance across exposure environments, degradation is notably more severe in sulfate conditions, as evidenced by higher weight loss (1.30–2.73% vs. 0.13–2.27%), greater compressive strength reduction (up to 20.84% loss in sulfate vs. 4.8% in chloride for Mi3Mt7.5), and more pronounced modulus decline (–4.05% in sulfate vs. +14.23% in chloride after 150 cycles, after adjustment

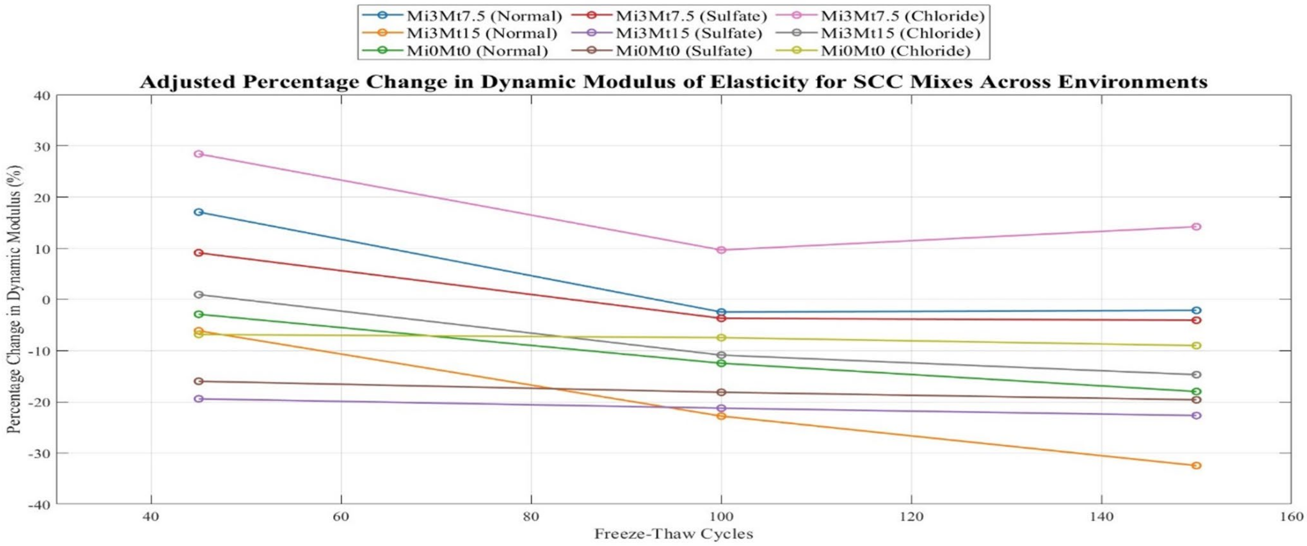

Fig. 11 Adjusted percentage change in dynamic modulus of elasticity for SCC mixes across environments

for age-related gains). This disparity arises from fundamental differences in degradation mechanisms: in sulfate environments, sulfate ions (SO_4^{2-}) react with calcium aluminate hydrates to form expansive ettringite and gypsum, inducing internal tensile stresses, microcracking, and volumetric expansion that exacerbate freeze–thaw damage. SEM analysis (Fig. 11) confirms this, showing extensive ettringite needle-like crystals in sulfate-exposed samples, leading to porosity up to 11.3% in the control mix compared to 5.1% in Mi3Mt7.5. In contrast, chloride environments primarily involve diffusive Cl^- penetration, which—in unreinforced concrete—causes less expansive disruption but facilitates gradual leaching of hydration products. This yields milder physical deterioration, allowing pozzolan-modified mixes like Mi3Mt7.5 to even exhibit net strength and modulus gains during early exposure, as ongoing pozzolanic reactions temporarily outpace damage accumulation.

The role of the air-entraining admixture (Fabair-200, fixed at 0.9 g/m³) is critical to these outcomes, facilitating controlled air voids (4–6% per ASTM C231 (2026) that mitigate hydraulic pressure during freezing (Tuncer et al. 2025; Patel and Shah 2013). This dosage contributed significantly to the low weight loss and high modulus retention in Mi3Mt7.5, particularly in chloride environments, where the stable air void system complemented the dense microstructure (porosity 4.2–5.1%). In sulfate environments, air voids helped accommodate ice expansion but were less effective due to chemical attack exacerbating microcracking. Notably, in high-metakaolin mixes like Mi3Mt15, the fixed air-entraining dosage was less effective due to increased viscosity, reducing air void stability and resulting in slightly lower air content (~4.2% vs. 5.1% in Mi3Mt7.5), which contributed to higher porosity (8.2–11.3%) and greater susceptibility to damage (Chithra 2022; Ashteyat et al. 2024). This interaction underscores the need for tailored air-entraining dosages in high-pozzolan mixes—a consideration for future studies.

Chemical durability metrics, such as reduced permeability inferred from low weight loss and SEM observations of denser matrices, build on Chithra (2022), who reviewed metakaolin's role in improving chloride resistance in SCC but without quantifying combined effects. Our outperformance in chloride (9.26% strength gain) differentiates from Abed and Balázs (2022), where SCMs showed variable freeze–thaw resistance. The novelty here is the simultaneous exposure to freeze–thaw, sulfate, and chloride—underexplored in prior works like Malaiškienė and Jakubovskis (2025) or Balamuralikrishnan and Saravanan (2021)—revealing that Mi3Mt7.5 mitigates ettringite formation more effectively than single-pozzolan systems, promoting sustainability through 10.5% cement reduction and associated CO_2 savings.

The incorporation of 3% micro-silica and 7.5% metakaolin not only enhances performance but also contributes significantly to sustainability. By replacing 10.5% of Portland cement, this mix reduces CO_2 emissions by approximately 94.5 kg/m³ (assuming 0.9 t CO_2/t cement and 900 kg/m³ cementitious content). Over a 10,000 m³ bridge deck, this equates to 945 tons of CO_2 saved—comparable to removing 200 passenger cars from the road for a year. From a life-cycle perspective, the enhanced durability (0.13–1.30% mass loss; 93.3% modulus retention) extends service life, reducing repair frequency and embodied carbon from maintenance. Compared to Gyurkó et al. (2019), who used cellular concrete waste without combined exposure testing, the

Mi3Mt7.5 mix ensures longer-lasting structures with lower lifecycle emissions.

The enhanced durability of Mi3Mt7.5 has significant implications for real-world infrastructure. In bridge decks and pavements exposed to de-icing salts, the sustained compressive strength (53.43–62.29 MPa after 150 cycles) could extend service life by 20–50 years. For marine piles in sulfate–chloride environments, suppressed ettringite formation and denser microstructure (porosity 4.2–5.1%) doubles service life from 50 to 100 to 100–200 years. The choice of 7.5% metakaolin is justified by dosage-dependent effects: at this level, metakaolin maximizes pore refinement and chemical resistance through balanced pozzolanic reactions, while higher dosages (e.g., 15%) lead to agglomeration, reduced homogeneity, and increased cracking susceptibility (Chithra 2022; Ashteyat et al. 2024). This dosage ensures optimal synergy with 3% micro-silica, resulting in a 35% reduction in large pores and enhanced sustainability benefits.

Collectively, these findings affirm that optimal, not maximal, use of supplementary cementitious materials is essential for achieving high performance under complex environmental stressors. The Mi3Mt7.5 formulation exemplifies this balance, offering exceptional resilience in chloride-rich settings and robust—though not immune—performance in aggressive sulfate environments, thereby providing a practical, sustainable solution for cold, coastal, and saline infrastructure applications.

5 Conclusion

This study, through its investigation of the effects of freeze–thaw cycles on self-compacting concrete (SCC) incorporating micro-silica and metakaolin in sulfate and chloride environments, provides valuable insights into enhancing the durability and performance of concrete structures under harsh conditions. By addressing the research gap concerning the combined effects of micro-silica and metakaolin under simultaneous freeze–thaw, sulfate, and chloride exposure, this research offers novel insights into the performance of SCC in complex environmental conditions. The main innovation of this work is the optimization of the 3% micro-silica and 7.5% metakaolin blend (Mi3Mt7.5), which simultaneously improves both mechanical properties and durability of SCC while enhancing sustainability through reduced cement consumption and lower CO_2 emissions. The key findings of this study are summarized as follows:

1. The simultaneous use of micro-silica and metakaolin—particularly in the optimized Mi3Mt7.5 blend—represents the key innovation of this study, significantly enhancing both mechanical performance and durability of SCC. This combination increases resistance to freeze–thaw deterioration by reducing porosity and promoting the formation of resilient C-S-H and C-A-H gels, while also supporting sustainability by minimizing cement usage and CO_2 emissions.
2. The Mi3Mt7.5 mix exhibited the highest compressive strength (62.29 MPa after 150 cycles) and dynamic modulus of elasticity (45.62 GPa) in a chloride environment, with minimal weight loss (0.13%), demonstrating exceptional resistance to chloride penetration and freeze–thaw damage.
3. In sulfate environments, the Mi3Mt7.5 mix achieved a compressive strength of 53.43 MPa and low weight loss (1.30% after 150 cycles), outperforming other mixes. Scanning electron microscopy (SEM) analysis confirmed reduced ettringite crystal formation—a key factor in sulfate-induced deterioration.
4. The Mi3Mt15 mix (3% micro-silica and 15% metakaolin) displayed the lowest compressive strength (45.14 MPa in sulfate environments) and dynamic modulus (28.09 GPa in sulfate environments) due to excessive viscosity and reduced compaction, underscoring the importance of optimizing additive dosages.
5. The reduction in weight loss from 2.27 to 2.73% at 28 days (45 cycles) to 1.05–1.30% at 90 days (150 cycles) in the Mi3Mt7.5 mix indicates enhanced durability due to completed hydration processes and increased cement matrix densification.
6. The findings highlight the suitability of the Mi3Mt7.5 mix for concrete structures in cold and corrosive settings, such as marine structures and pavements exposed to de-icing salts, contributing to extended service life and sustainability. This approach also reduces the environmental impact by lowering CO_2 emissions associated with cement production.
7. By providing comprehensive experimental data and microstructural analyses, this study offers a valuable reference for designing high-performance concrete and supports the development of engineering standards for structures in challenging environments.

However, this study has notable limitations. The use of 100 mm cubic specimens, necessitated by laboratory equipment constraints, influenced compressive strength results, as cubic specimens typically yield 5–15% higher strengths than standard 150 mm × 300 mm cylinders due to reduced edge effects and confinement. This could lead to an overestimation of absolute strength values, though relative comparisons among mixes remain valid. Additionally, the absence of rapid chloride permeability tests (RCPT) and sulfate expansion tests limits insights into long-term ion penetration and volumetric stability. The limited number of specimens tested, due to laboratory constraints, also affects the statistical robustness of the results. For future research, incorporating numerical modeling, field validation, and life-cycle cost analyses is recommended to further evaluate the Mi3Mt7.5 blend's long-term performance and economic benefits. This study provides a practical framework for designing durable SCC in severe conditions, emphasizing the role of optimized pozzolanic blends in enhancing performance and sustainability.

Author contributions Conflict of Interest and Authorship Confirmation FormPlease check the following as appropriate: All authors have participated in (a) conception and design, or analysis and interpretation of the data; (b) drafting the article or revising it critically for important intellectual content; and (c) approval of the final version.This manuscript has not been submitted to, nor is under review at, another journal or other publishing venue.The authors have no affiliation with any organization with a direct or indirect financial interest in the subject matter discussed in the manuscript.All persons who meet authorship criteria are listed as authors and all authors certify that they have participated sufficiently in the work to take public responsibility for the content, including participation in the concept, design, analysis, writing, or revision of the manuscript. Furthermore, each author certifies that this material or similar material has not been and will not be submitted to or published in any other publication before its appearance in the Iranian Journal of Science and Technology, Transactions of Civil Engineering.1. Yaghoub Mohammadi, Professor, Department of Civil Engineering, Faculty of Engineering, University of Mohaghegh Ardabili, Ardabil, Iran, yaghoubm@uma.ac.ir2. Arian DarvishaliNezhad, PhD (c) of Structural Engineering, Department of Civil Engineering, Faculty of Engineering, University of Mohaghegh Ardabili, Ardabil, Iran, arian.darvishalinezhad@uma.ac.ir3. Husain Khalaf Jarallah, Assistant Professor, Department of Civil Engineering, College of Engineering, Mustansiriyah University, Baghdad, Iraq, khalfdce@uomustansiriyah.edu.iqAll persons who meet authorship criteria are listed as authors, and all authors certify that they have participated sufficiently in the work to take public responsibility for the content, including participation in the concept, design, analysis, writing or revision of the manuscript. Furthermore, each author certifies that this material or similar material has not been and will not be submitted to or published in any other publication before its appearance in the Iranian Journal of Science and Technology, Transactions of Civil Engineering.1. Yaghoub Mohammadi: Methodology, Validation, Formal analysis, Investigation, Resources, Data Curation, Writing - Original Draft, Writing - Review & Editing and Visualization.2. Arian DarvishaliNezhad: Conceptualization, Methodology, Validation, Formal Analysis, Investigation, Resources, Data Curation, Writing - Original Draft, Writing - Review & Editing, Visualization and Supervision.3. Husain Khalaf Jarallah: Methodology, Validation, Formal Analysis, Investigation, Resources, Data curation, Writing - Original Draft, Writing - Review & Editing and Visualization.

Funding This research did not receive any specific grant from funding agencies in the public, commercial, or not-for-profit sectors.

Data Availability No datasets were generated or analysed during the current study.

Declarations

Competing interests The authors declare no competing interests.

References

Abbas MM, Muntean R (2025) The effectiveness of different additives on concrete's freeze–thaw durability: a review. Materials 18(5):978. https://doi.org/10.3390/ma18050978

Abbas R, Abo-El-Enein SA, El-Sayed E (2010) Propiedades y durabilidad del cemento con adición de metacaolín: mortero y hormigón. Materiales de construcción 60(300):33–49. https://doi.org/10.3989/mc.2010.50609

Abdellatief M, Elsafi M, Murali G, ElNemr A (2025) Comparative evaluation of hybrid machine learning models for predicting the strength of metakaolin-based geopolymer concrete enhanced with Gaussian noise augmentation. J Build Eng 113302. https://doi.org/10.1016/j.jobe.2025.113302

Abdellatief M, Hassanien AE, Mortagi M, Hamouda H (2025) Geopolymer foam concrete: a review of pore characteristics, compressive strength, and artificial intelligence in GFC strength simulations. Discover Concrete Cem 1(1):4. https://doi.org/10.1007/s44416-025-00003-x

Abdellatief M, Abd-Elmaboud ME, Mortagi M, Saqr AM (2025) A convolutional neural network-based deep learning approach for predicting surface chloride concentration of concrete in marine tidal zones. Sci Rep 15(1):27611. https://doi.org/10.1038/s41598-025-12035-1

Abed MA, Balázs GL (2022) Regions: understanding concrete's resistance to freezing/thawing. Sustain Concr Synth Recycl Aggr. https://doi.org/10.5772/intechopen.99968

American Concrete Institute (1977) Recommended practice for selecting proportions for normal and heavyweight concrete; (ACI 211.1–77) Detroit. American Concrete Institute, Farmington Hills, MI, USA

Ashteyat A, Obaidat AT, Qerba'a R, Abdel-Jaber MT (2024) Influence of basalt fiber on the rheological and mechanical properties and durability behavior of self-compacting concrete (SCC). Fibers Basel 12(7):52. https://doi.org/10.3390/fib12070052

ASTM C127-24 (2025) Standard test method for relative density (specific gravity) and absorption of coarse aggregate. ASTM International, West Conshohocken

ASTM C128-22 (2025) Standard test method for relative density (specific gravity) and absorption of fine aggregate. ASTM International, West Conshohocken

ASTM C131/C131M-20 (2020) Standard test method for resistance to degradation of small-size coarse aggregate by abrasion and impact in the los angeles machine. ASTM International, West Conshohocken

ASTM C136/C136M-19 (2020) Standard test method for sieve analysis of fine and coarse aggregates. ASTM International, West Conshohocken

ASTM C192/C192M-25 (2025) Standard practice for making and curing concrete test specimens in the laboratory. ASTM International, West Conshohocken

ASTM C231/C231M-22 (2026) Standard test method for air content of freshly mixed concrete by the pressure method. ASTM International, West Conshohocken

ASTM C260/C260M-10a (2025) Standard specification for air-entraining admixtures for concrete. West Conshohocken

ASTM C33/C33M-18 (2023) Standard specification for concrete aggregates. ASTM International, West Conshohocken

ASTM C39/C39M-21 (2025) Standard test method for compressive strength of cylindrical concrete specimens

ASTM C494/C494M-24 (2024) Standard specification for chemical admixtures for concrete. ASTM International, West Conshohocken

ASTM C535-16 (2024) Standard test method for resistance to degradation of large-size coarse aggregate by abrasion and impact in the los angeles machine. ASTM International, West Conshohocken

ASTM C597-22 (2023) Standard test method for ultrasonic pulse velocity through concrete. ASTM International, West Conshohocken

ASTM C666/C666M-15 (2024) Standard test method for resistance of concrete to rapid freezing and thawing. ASTM International, West Conshohocken

ASTM D1129-13 (2024) Standard terminology relating to water. ASTM International, West Conshohocken

ASTMC 330–87 (1982) Standard specification for lightweight aggregate for structural concrete. Annual book ASTM Stand 4(2):112–118

Balamuralikrishnan R, Saravanan J (2021) Effect of addition of alccofine on the compressive strength of cement mortar cubes. Emerg Sci J 5(2):155–170. https://doi.org/10.28991/esj-2021-01265

Bhavani K, Saravanan M (2023) Strength properties and sulphate resistance of self-compacting concrete incorporating silica fume and metakaolin. Innovations 74:49–58. https://doi.org/10.54882/74202374112320

Bogdanov R, Mavlyuberdinov A (2020) Development of the composition of the self-compacting concrete with high performance. In IOP conference series: Materials Science and Engineering (Vol. 890, No. 1, p. 012132). IOP Publishing. https://doi.org/10.1088/1757-899X/890/1/012132

Bumanis G, Bajare D (2017) The effect of curing conditions on the durability of high-performance concrete. In IOP Conference Series: Materials Science and Engineering (Vol. 251, No. 1, p. 012006). IOP Publishing. https://doi.org/10.1088/1757-899X/251/1/012006

Chen Y, Waheed MS, Iqbal S, Rizwan M, Room S (2024) Durability properties of macro-polypropylene fiber reinforced self-compacting concrete. Materials 17(2):284. https://doi.org/10.3390/ma17020284

Chithra CJ (2022) A review on study of partial replacement of cement by metakaolin and glenium b233 in self-compacting concrete. Sustainability. https://doi.org/10.7770/safer-V10N1-art2468

Dhabhai S, Shekhawat RS (2020) Optimized concrete paver blocks utilizing micro silica as a partial replacement of cement. Int J Tech Res Sci 5(10):30–37. https://doi.org/10.30780/IJTRS.V05.I10.005

EN 12350-2:2009 (2009) Testing fresh concrete – Part 2: Slump-test

Ezhilarasi R, Reya George K (2020) Experimental investigation on self-compacting concrete by replacing industrial waste materials. Int J Eng Res Technol. https://doi.org/10.17577/IJERTV9IS050496

González-Sánchez JF, Taşcı B, Fernández JM, Navarro-Blasco Í, Alvarez JI (2020) Combination of polymeric superplasticizers, water repellents and pozzolanic agents to improve air lime-based grouts for historic masonry repair. Polymers Basel 12(4):887. https://doi.org/10.3390/polym12040887

Gyurkó Z, Szijártó A, Nemes R (2019) Cellular concrete waste as an economical alternative to traditional supplementary cementitious materials. J Therm Anal Calorim 138(2):947–961. https://doi.org/10.1007/s10973-019-08303-8

He J, Huang Z, Wang X, Xin M, Zhang Y, Lu H (2024) Advances in highly ductile concrete research. Materials 17(18):4596. https://doi.org/10.3390/ma17184596

Kabay N, Kizilkanat A, Tufekci M (2016) Effect of pre-wetted pumice aggregate addition on concrete properties under different curing conditions. Period Polytech Civ Eng. https://doi.org/10.3311/PPCI.7767

Khosravi H, Toloue-Hassanpour MR, Lezgy-Nazargah M (2025) Investigating the effects of nano-materials on the mechanical and durability properties of self-consolidating concrete. CivilEng 6(1):12. https://doi.org/10.3390/civileng6010012

Li H, Guo H, Zhang Y (2022) Deterioration of concrete under the coupling action of freeze–thaw cycles and salt solution erosion. Reviews Adv Mater Sci 61(1):322–333. https://doi.org/10.1515/rams-2022-0025

Li Y, Zhang L, Ma C, Li B, Zhu J (2020) Damage mechanism of mineral admixture concrete under marine corrosion and freezing-thawing environment. Adv Civ Eng 2020(1):8817113. https://doi.org/10.1155/2020/8817113

Liu F, You Z, Xiong R, Yang X (2021) Effects of Sodium Sulfate attack on concrete incorporated with drying-wetting cycles. Adv Civ Eng 2021(1):5393504. https://doi.org/10.1155/2021/5393504

Luan C, Zhang Q, Wu Z, Han Z, Zhou Z, Du P, Wu F, Huang Y (2023) Uncovering the role of hydrophobic silica fume (HPS) in rheology, hydration, and microstructure of ultra-high-performance concrete (UHPC). J Sustainable Cement-Based Mater 12(11):1399–1413. https://doi.org/10.1080/21650373.2023.2222398

Malaiškienė J, Jakubovskis R (2025) Influence of pozzolanic additives on the structure and properties of ultra-high-performance concrete. Materials 18(6):1304. https://doi.org/10.3390/ma18061304

Moceikis R, Kičaitė A, Sahmenko G, Selsekienė A (2020) Durability characterisation of glass fibre reinforced concrete by resistance to freezing and thawing. J Sustainable Archit Civil Eng 26(1):98–109. https://doi.org/10.5755/j01.sace.26.1.25130

Mousavi SS, Bhojaraju C, Ouellet-Plamondon C (2021) Clay as a sustainable binder for concrete—a review. Constr Mater 1(3):134–168. https://doi.org/10.3390/constrmater1030010

Müller M, Ludwig HM, Hasholt MT (2021) Salt frost attack on concrete: the combined effect of cryogenic suction and chloride binding on ice formation. Mater Struct 54(5):189. https://doi.org/10.1617/s11527-021-01779-7

Naresh T, Mallik M, Venkateswara Rao S, Dubey S (2025) Performance and microstructural optimization of sustainable geopolymer mortars using fly ash, ground granulated blast furnace slag, and rice husk ash. Struct Concrete. https://doi.org/10.1002/suco.70192

Naresh T, Mallik M, Venkateswara Rao S, Dubey S (2025) Advanced statistical optimization and performance evaluation of self-compacting geopolymer concrete utilizing industrial by-products. Struct Concrete. https://doi.org/10.1002/suco.70092

Okamura H, Ouchi M (2003) Self-compacting concrete. J Adv Concr Technol 1(1):5–15

Patel V, Shah N (2013) A survey of high-performance concrete developments in civil engineering field. Open J Civ Eng 3(2):69–79. https://doi.org/10.4236/ojce.2013.32007

Penna R, Feo L, Martinelli E, Pepe M (2022) Theoretical modelling of the degradation processes induced by freeze–thaw cycles on bond-slip laws of fibres in high-performance fibre-reinforced concrete. Materials 15(17):6122. https://doi.org/10.3390/ma15176122

Skripkiūnas G, Nagrockienė D, Kerienė JR, Janavičius E, Girskas G, Špokauskas AA (2013) Microstructure changes in hardened cement paste after freezing-thawing cycles. https://doi.org/10.5755/J01.MS.19.1.3835

Thatikonda N, Mallik M, Rao SV, Dubey S (2025) Performance and microstructural characterization of sustainable self-compacting geopolymer concrete with multi-component binders. Sust Chem Pharm 44:101926. https://doi.org/10.1016/j.scp.2025.101926

Thatikonda N, Mallik M, Madduru SVR, S., R., C.,T., R., K., D (2024) Influential studies on microsilica as a potential replacement for fly ash-GGBFS in self-compacting geopolymer concrete: Microstructural insights and performance analysis. J Building Pathol Rehabilitation 9(1):66. https://doi.org/10.1007/s41024-024-00422-6

Tuncer M, Bideci A, Çomak B, Durmuş G, Bideci ÖS (2025) Experimental investigation of durability properties of polymer-coated pumice aggregate lightweight concretes. Polymers 17(2):253. https://doi.org/10.3390/polym17020253

Wang R, Zhang Y, Wu H, Jiang X (2025) Study on the influencing factors of UHPC durability and its microscopic performance characterization. Materials 18(14):3268. https://doi.org/10.3390/ma18143268

Xiong J, Su D, Wang S, Li P, Zhang X, Zhang Z, Zhong M (2023) Influence of the Coupling Action of Flexural Load and Freezing–Thawing on the Chloride Diffusion of Marine High-Performance Concrete. Buildings 13(2):325. https://doi.org/10.3390/buildings13020325

Yan M (2024) Research on the variation law of compressive strength of concrete under the coupling effect of freeze–thaw and salt corrosion. Academic Journal of Science and Technology. https://doi.org/10.54097/ttxm1d14

Zhagifarov AM, Akhmetov DA, Suleyev DK, Zhumadilova ZO, Begentayev MM, Pukharenko YV (2024) Investigation of hydrophysical properties and corrosion resistance of modified self-compacting concretes. Materials Basel 17(11):2605. https://doi.org/10.3390/ma17112605

Zhao R, Shi C, Zhang R, Wang W, Zhu H, Luo J (2024) Study on the freeze–thaw resistance of concrete pavements in seasonally frozen regions. Materials 17(8):1902. https://doi.org/10.3390/ma17081902